

Quaternary Faulting and Seismic Source Characterization in the El Paso-Juarez Metropolitan Area; Collaborative Research with the University of Texas at El Paso

Program Element II: Evaluate Urban Hazard and Risk.

Final Technical Report
Contract 03HQGR0056
National Earthquake Hazards Reduction Program
U.S. Geological Survey

Principal Investigator:
James P. McCalpin
GEO-HAZ Consulting, Inc.
P.O. Box 837, 600 E. Galena Ave.
Crestone, CO 81131
OFFICE: (719) 256-5227
FAX: (719) 256-5228
www.geohaz.com/geohaz

26 April 2006

This report was prepared under contract to the U.S. Geological Survey and has not been reviewed for conformity with USGS editorial standards and stratigraphic nomenclature. Opinions and conclusions expressed herein do not necessarily represent those of the USGS. Any use of trade names is for descriptive purposes only and does not imply endorsement by the USGS.

TABLE OF CONTENTS

1. ABSTRACT.....	4
2. INTRODUCTION.....	5
2.1 Purpose and Scope of Study.....	5
2.2 Significance of the project.....	5
2.3 Geomorphology and General Geology of the Franklin Mountains.....	6
2.3.1 Quaternary Geology and Neotectonics	11
3. METHODS	12
4. EAST FRANKLIN MOUNTAINS FAULT STUDY SITE	14
4.1 The NEHRP 1995 Study of the East Franklin Mountains Fault.....	14
4.2 This Study (NEHRP 2003) of the East Franklin Mountains Fault—Overview	18
4.3 2003 Primary Trench Site.....	20
4.3.1 Geomorphology	20
4.3.2 Stratigraphy	21
4.3.3 Soils	27
4.3.4 Structure.....	28
4.3.5 Geochronology	32
4.4 Interpretation of Primary Trench Site	35
4.4.1 Number of Paleearthquake Events Interpreted.....	35
4.4.2 Displacement Per Event.....	36
4.4.3 Recurrence Interval Between Paleearthquakes	37
4.4.4 Slip Rates	38
4.5 2003 Arroyo Exposure	39
4.5.1 Geomorphology.....	39
4.5.2 Stratigraphy	40
4.5.3 Soils	40
4.5.4 Structure.....	40
4.6 Interpretation	40
5. SEISMIC SOURCE CHARACTERISTICS OF THE EAST FRANKLIN MOUNTAINS FAULT	42
5.1 Number of Paleearthquake Events Interpreted.....	42
5.2 Displacement Per Event.....	42
5.3 Recurrence Interval Between Paleearthquakes	42
5.4 Slip Rates	42
5.5 Implications for Regional Seismic Hazards	43
6. CONCLUSIONS	44
7. REFERENCES	45
8. ACKNOWLEDGMENTS	48
9. APPENDIX 1; Characteristics of the East Franklin Mountains fault, from USGS Quaternary Fault and Fold Database.....	49
9. APPENDIX 2; Structure of the Franklin Mountains (from Richardson, 1909).....	55
9. APPENDIX 3; RADIOCARBON DATES	58
9. APPENDIX 4; Pollen analysis of Unit 13Kb3 from Primary Trench.....	61
PLATE 1; Log of the 2003 primary trench (in pocket)	

List of Figures	Page
Fig. 1. Generalized map of faults in the El Paso region (from Keaton and Barnes, 1996)	8
Fig. 2. Location map of the East Franklin Mountains and its boundary faults	9
Fig. 3. Schematic cross-section across the Hueco Bolson and Hueco graben.....	9
Fig. 4. Aerial photograph of the East Franklin Mountains, looking north from over the City of El Paso.....	10
Fig. 5. Photograph of the piedmont fault scarps of the East Franklin Mountains fault.....	13
Fig.6. Sketch map of the EFMF and subsidiary fault traces in the Hueco graben, from Keaton and Barnes (1996)	15
Fig. 7. Location map of trench and arroyo exposure, from Keaton and Barnes (1996).....	16
Fig. 8. Log of the north wall of the primary trench of Keaton and Barnes (1996).....	17
Fig. 9. Annotated map of driving directions to the 2003 trench and arroyo exposure	18
Fig. 10. Photo of the uppermost (western) part of the 1995 trench taken in March 2003, before our reexcavation.....	19
Fig. 11. Photo of the lower (eastern) part of the 1995 trench taken in March 2003, before our reexcavation.....	19
Fig. 12. Telephoto view of the ca. 8 m-high fault scarp across the Jornada II alluvial fan surface at the primary trench site, which is visible at far right as a spoil pile and orange fencing.....	20
Fig. 13. Annotated field log of the footwall of the main fault, on the North Wall.....	22
Fig. 14. Photo of footwall on N trench wall, centered on the upper part of fault D.....	23
Fig. 15. Plot of delta O ¹⁸ in marine sediments, from Imbrie et al. (1992)	27
Fig. 16. Photo of the upper (graben) part of the main fault zone (fault C) on the south wall	30
Fig. 17. Photo of the lower 2 m of fault E (between red flagging on wall) on the north trench wall	31
Fig. 18. Vertical displacement as a function of deposit age, adapted from Keaton and Barnes (1996)	38
Fig. 19. Photo of the arroyo exposure after deepening along the fault zone	39
Fig. 20. Photomosaic of the arroyo exposure	41
Fig. 21. Vertical displacement as a function of deposit age, adapted from Keaton and Barnes (1996)	43

List of Tables

Table 1. Fault parameters used in the 2002 version of the US National Seismic Hazard Map.	6
Table 2. Unit descriptions on the hanging wall and in the main fault zone.....	25
Table 3. Summary of 15 radiocarbon samples collected and 3 dated	32
Table 4. Summary of multi-aliquot infrared-stimulated luminescence measurements on the fine silt fraction.....	34
Table 5. Estimated displacements per event in the EFMF primary trench	37

1. ABSTRACT

Our reexcavation of Keaton and Barnes' (1996) primary trench across the EFMF resulted in a different interpretation of fault displacement and age. Our luminescence age estimates, as well as sedimentology, indicate that the hanging-wall stratigraphy is only about half as old as assumed by Keaton and Barnes (1996), and only half as old as the footwall stratigraphic sequence. This is because the hanging wall of the fault scarp has been buried by younger alluvium, so the height of the scarp is considerably less than the net vertical displacement of the footwall stratigraphic units. We believe that this is a pervasive phenomenon along the EFMF, and has been generally unrecognized by previous workers, who equated scarp height with net displacement. We further believe that the reason for pervasive fluvial burial of the downthrown block is because the fault traces of the EFMF commonly lie 1 or more miles valleyward of the range front, and traverse a low-gradient piedmont. Thus the ephemeral streams have a low enough gradient that they tend to deposit alluvium and to fill up any tectonic "hole" (accommodation space) that might be created by normal faulting.

Because there is no correlation of strata across the fault, our net vertical displacement estimate is >11.2 m, compared to Keaton and Barnes (1996) estimate of 9.2-9.4 m. As a result of our larger displacement and much younger age, our calculated slip rate at the primary trench is 0.18 mm/yr, compared to their rate of 0.10 mm/yr.

Fault scarp heights and drillhole data provide first-approximations of vertical displacement across older datums (250-400 ka, 400-500 ka), but these approximations are also minimum values. The post-500 ka average slip rate based on these datums is 0.145 mm/yr.

We recommend that the next version of the National Seismic Hazard Map use the following slip rates for the EFMF: 0.145 mm/yr (weighted 65%) and 0.18 mm/yr (weighted 35%).

2. INTRODUCTION

2.1 Purpose and Scope of Study

This report summarizes trenching and dating results on the East Franklin Mountains fault (EFMF) from April of 2003, in a continuing effort to characterize the mid-late Quaternary activity of normal faults in the Rio Grande rift near El Paso, Texas. In particular, this study continues efforts begun in FY95 (Keaton et al., 1995; Keaton and Barnes, 1996) to derive a Paleoearthquake chronology and magnitude estimates for the EFMF (Fig. 1).

The fault scarps of the EFMF trend north-south and face east, traversing the head of a middle Pleistocene (?) pediment at the base of the East Franklin Mountains (Fig. 2). During March and April of 2003 we spent 4 weeks excavating, logging, and sampling one trench and one arroyo bank on the northern end of the EFMF (Fig. 3). The trench was basically a deepening and lengthening of Keaton and Barnes' (1996) trench, which was still open in March of 2003. We felt that reexcavating this trench would provide the maximum return of geologic information for the cost, which was limited in our budget. In addition to the trench, we deepened, cleaned, and logged a natural exposure of the EFMF in an arroyo streambank about 3.5 km north of the trench (Fig. 3).

The goal of this trenching investigation was to reconstruct the chronology of surface-faulting events on the EFMF since the abandonment of the middle Pleistocene pediment as a depositional surface, and to estimate the parameters of characteristic earthquake magnitude, slip rate, and recurrence interval.

2.2 Significance of the project

Prior to this study, only one detailed paleoseismic study had been performed on the EFMF (Barnes et al., 1995; Keaton et al., 1995; Keaton and Barnes, 1996). Based on this study and on the fault length, the Quaternary Fault and Fold Database of the US characterizes the EFMF as follows:

Length:	52.7 km
Scarp Heights:	2-60 m
Date of MRE:	10.9 ka
Date of PE:	>15.6 ka
Recurrence Interval:	9-22 ky in temporal clusters; 75-100 ky between clusters
Slip Rate:	0.1 mm/yr (averaged over past 130 ka) to 0.3 mm/yr (within cluster)

The fault length, if assumed equal to surface rupture length, would imply a Characteristic Earthquake magnitude of $M7.1 \pm 0.3$ (Wells and Coppersmith, 1994, normal fault data).

The EFMF was not included on the 1996 National Seismic Hazard Map as a line source of ground motion, which is understandable because Keaton and Barnes' (1996) initial study was not yet available. However, the EFMF was added to the US National Seismic Hazard Map (2002 version) as a fault line source with the following parameters (Table 1):

Table 1. Fault parameters used in the 2002 version of the US National Seismic Hazard Map. From http://gldims.cr.usgs.gov/webapps/cfusion/Sites/C2002_Search/index.cfm

Name	State	Slip rate (mm/yr)	Dip (degrees)	Rupture top (km)	Width (km)	Char Mag ¹	Char Rate ¹	Effective Date
East Franklin Mountains fault	Texas	0.1	60	0	17	7	8.15E-05	08/19/2004

The USGS Characteristic Magnitude (M=7) is slightly smaller than the magnitude implied by the fault length (M=7.1±0.3). The USGS “characteristic rate” of 0.0000815/yr equates to a recurrence interval between characteristic earthquakes of 12,270 yrs. It is not clear exactly how this value was computed, since it is different than the recurrence intervals computed by Keaton et al. (1995) of “9-22 ky in temporal clusters; 75-100 ky between clusters.”

2.3 Geomorphology and General Geology of the Franklin Mountains

Rising over 1000 m above the surrounding basins, the Franklin Mountains dominate the skyline of the city of El Paso. The range begins within the El Paso City limits in the south and extends northward across the New Mexico border for a distance of about 24 km. The Franklins are the southernmost extension of an almost continuous series of north-south trending ranges that extend over 160 km. The ranges include, from north to south: the San Andres, San Augustine, Organ (all in New Mexico), North Franklin, and Franklin ranges.

The continuous north-south ridge line of the Franklin and North Franklin mountains is separated by Anthony Gap approximately 0.8 km north of the New Mexico state line. The 11 km long North Franklin Mountains are separated from the Organ Mountains by the 7.2 km Fillmore Pass (elevation 1284 m). The ancestral Rio Grande once flowed through this pass and into the Hueco Basin, prior to the stream piracy that diverted the river to its current position west of the range.

Richardson (1909) described the general physiography as follows: *“The Franklin Mountains are the southern extremity of the long, narrow chain that extends from the termination of the main mass of the Rocky Mountains, in northern New Mexico, southward as far as El Paso. This chain occupies a belt about 10 miles wide and 250 miles long across central New Mexico immediately east of the Rio Grande valley. Its continuity is broken in places, causing a separation into several units known as the Sandia, Manzano, Oscura, San Andreas, and Franklin ranges, named in order from north to south. The Franklin Range trends slightly west of north and extends from El Paso to a point a few miles north of the New Mexico-Texas boundary, where it is separated by a low wash-filled pass from the Organ Mountains, which form the southern extremity of the San Andreas Range.*

The main part of the Franklin Range lies entirely within Texas and is 15 miles long and about 3 miles wide, but low outlying hills extend the range 8 miles beyond the State boundary. The mountains rise abruptly more than 3000 feet above the Rio Grande valley on the west and the Hueco Bolson on the east, culminating in a peak 7152 feet above sea level. The western face of the range is relatively little eroded and in the main constitutes a dip slope; the eastern face, on the contrary, is more dissected and exposes cross sections of the rocks, deep valleys that extend back almost to the rim of the range separating several transverse ridges. Individuality is given to the topography by the varying character of the formations. The crest of the range, capped for the greater part of its length by westward-dipping limestone, presents a rugged scarp; the lower slopes and transverse ridges have characteristic irregular surfaces due to the varying resistance to weathering of the component rocks. The mountains are practically bare of vegetation save for a scanty desert growth on the lower slopes, so that the rocks are plainly exposed except where they are covered by accumulations of debris. As a whole, the Franklin Range resembles an eroded block mountain of the Basin Range type.”

Richardson (1909) described the general outline of the “STRUCTURE OF THE EL PASO DISTRICT as follows: *“The main structural features of the El Paso district may be summarized as follows: The long, narrow Franklin Range, rising 3000 feet above broad lowlands, resembles a "basin range" fault block of west ward-dipping rocks, but it differs from the type by being part of a long chain of ranges and by being complexly faulted internally. The Hueco Mountains in the main form a monocline of low eastward dip along the western border of which the rocks have been disturbed. In the northern part of the quadrangle the strata in the belt of low outlying bills west of the Hueco Mountains dip westward, marking an unsymmetrical anticline; farther south more complex conditions are indicated by dips in various directions. In the Hueco Bolson the deep cover of unconsolidated material conceals the structure of the underlying rocks. Possibly a large part of the area is underlain by practically flat-lying beds which are faulted near the western margin of the bolson along the eastern base of the Franklin Mountains.*

The structure of the Franklin Mountains viewed from a distance appears simple. The strata strike parallel to the trend of the range and dip westward at steep angles. But the simplicity is only apparent, for the distribution of the rocks shows that the range is traversed by many faults. As a whole the long, narrow mountain belt bordered by broad waste-covered deserts, the western slopes coinciding with the dip of the rocks and the steeper eastern face exposing eroded edges of the strata, presents the general appearance of an eroded fault block of the basin-range type.”

When discussing the eastern and western boundary faults of the Franklin Mountains, he states: *“The Franklin Range lies between two major longitudinal dislocations which separate it from the Hueco block on the east and the Anthony block on the west. On the east the position of the hypothetical fault along the base of the range [i.e., the EFMF] is completely concealed by wash.”* However, in another section of his monograph he states that Quaternary deposits are faulted along the EFMF (cited in next section).

The block faulting that created the Franklin Mountains is presumably Neogene, and followed the Sevier-Laramide compressive orogeny, as inferred by Richardson (1909): *“At the close of the*

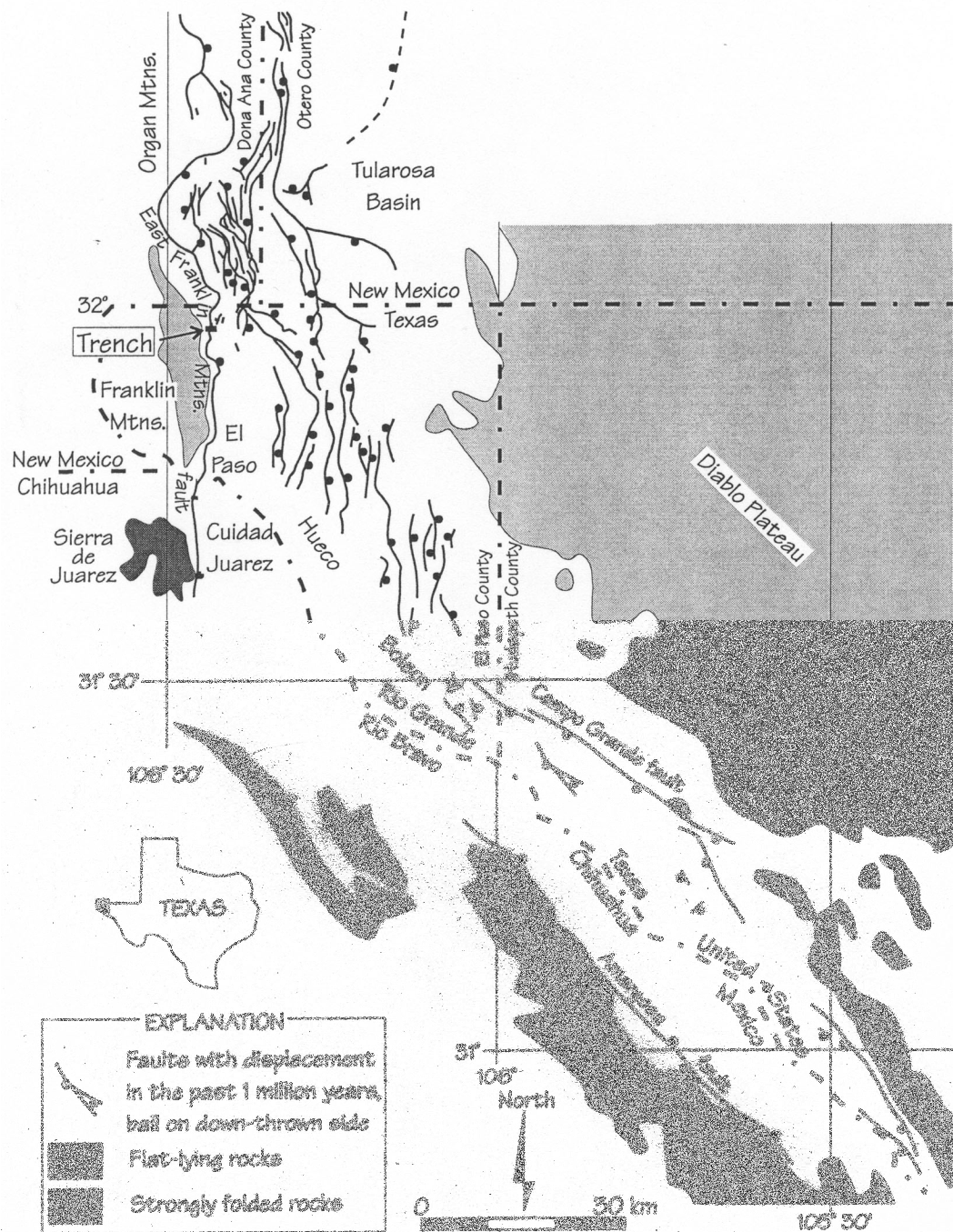


Fig. 1. Generalized map of faults in the El Paso region (from Keaton and Barnes, 1996). The East Franklin Mountains fault and trench site are at upper left.

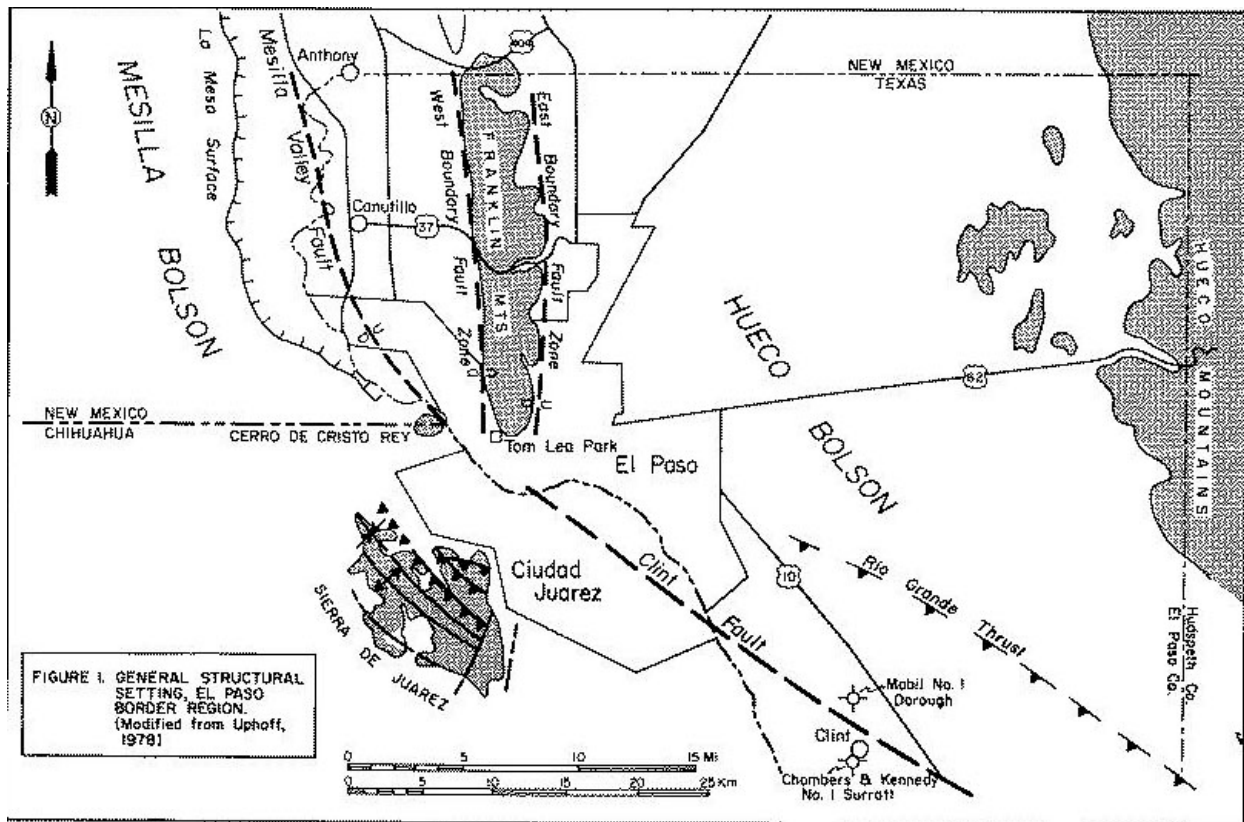


Fig. 2. Location map of the East Franklin Mountains and its boundary faults. To date, the West Boundary Fault has not been studied.

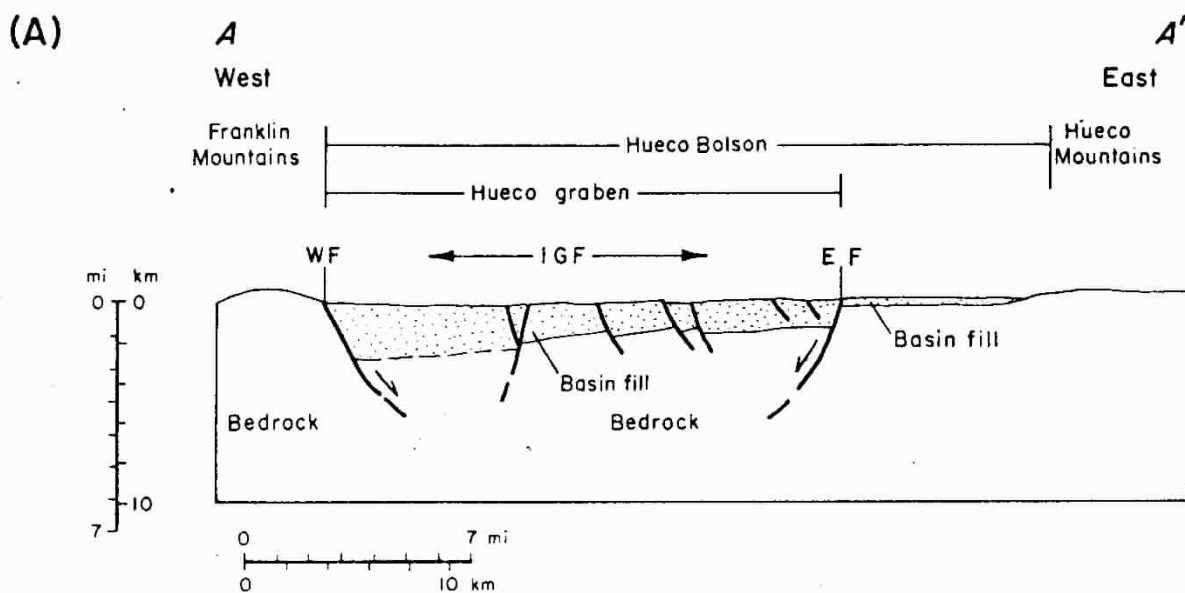


Fig. 3. Schematic cross-section across the Hueco Bolson and Hueco graben. The East Franklin Mountains fault (labeled as WF) forms the western margin of the graben. From Collins, 1999.



Fig. 4. Aerial photograph of the East Franklin Mountains, looking north from over the City of El Paso. Black blob at bottom is landing gear.

Cretaceous period or early in Tertiary time continental uplift and associated orogenic disturbances occurred throughout the Cordilleran region. The major deformation of the El Paso district probably developed during this period, when the mountain blocks and intervening basins were outlined. What little is known of the Tertiary history of the district implies that erosion of the recently uplifted land mass was the dominant process and was accompanied by local igneous intrusions and probably by continued uplift, both regional and differential. A great mass of Cretaceous and underlying rocks was removed from the highlands and at least part of the debris accumulated in the adjacent trough. The differential movement resulting in the uplift of the highlands above the basin was probably of long duration, progressing with the erosion of the uplands.

The Quaternary record of the district is one of continued erosion and deposition, accompanied by relatively minor uplift. Although the salient masses, the Franklin and Hueco mountains and the Hueco Bolson, are primarily of structural origin, they, have been much modified by erosion and deposition, which have formed the present mature topography. The highlands have been considerably reduced from their original forms, as shown in part by the well-developed drainage of the Franklin Mountains contrasted with the unsymmetrical drainage of tilted block mountains in a youthful stage; and the Hueco Bolson trough has been deeply filled to the present almost level plain by debris derived from the disintegration of the rocks of the highlands. Although many of the earlier deposits were probably laid down in water, the later material, constituting the uppermost bolson deposits, accumulated in large part under arid subaerial conditions. Detritus collects in the lowlands because the rainfall is insufficient to maintain streams that can convey the material to the river. The ultimate result of these conditions, if unchecked, will be the reduction of the area, to a plain.”

The EFMF defines the eastern margin of the East Franklin Mountains and the western margin of the Hueco Basin (or Bolson), a major topographic and structural basin of the Basin and Range extensional province in Texas. In a gross sense the Hueco Basin is an asymmetric west-tilted half graben (Fig. 4).

2.3.1 Quaternary Geology and Neotectonics

The Late Cenozoic basin and range faulting of the region probably initiated about Late Miocene (10 Ma). The bounding faults of the range indicate a Hueco bolson drop of 9000 ft (2744 m) on the east side of the range (Fig. x) and 10,000 ft (3049 m) along the western Mesilla Valley side.

The valley fill of the Hueco Bolson is variously named the Fort Hancock Formation (TX) or the Santa Fe Group (NM). Both names encompass the entire thickness of valley fill, beginning in the Miocene and continuing through the Pliocene. This valley fill is composed of subequal fluvial and lacustrine facies. In both TX and NM, different formation names are used for the uppermost part of the valley fill, spanning the latest Pliocene and the Pleistocene. In the Franklin Mountains area, this uppermost part of the section is termed the Camp Rice Formation (Plio-Pleistocene), and is distinguished as deposits related to the present Rio Grande. Its sedimentology is dominated by well-

stratified and well-sorted fluvial sand with subordinate gravel, deposited by a through-flowing Rio Grande.

Quaternary alluvial fan surfaces were subdivided by Gile et al. (1981) into Dona Ana (>400 ka), Jornada I (250-400 ka), Jornada II (25-150 ka), Isaack's Ranch (8-15 ka), and Organ I through III (7 ka to 100 yr BP). In the El Paso-Fort Bliss area, Monger (1993) later subdivided the Jornada II into a main phase (95-150 ka) and a late phase (25-65 ka). However, in their Figures 13 and 14, Keaton and Barnes (1996) show 3 phases of Jornada II, an early phase (120-150 ka), a middle phase (75-95 ka), and a late phase (25-65 ka). The difference is not explained.

In the Franklin Mountains, landsliding and subsurface gravity gliding occurred throughout the range, as a result of the late Cenozoic topographic relief created by the continuing structural uplift and westward tilting of the range surface. Lovejoy (1975) indicates the presence of some 17 gravity glide and landslide brecciated and non-brecciated masses in the Franklins. He interprets the gliding features to be older and primarily confined to the east side of the range (north to south: Pipeline, Anthony's Nose, and Taylor Block gravity glides). Landslides seem to have occurred more recently and on both sides of the range. Examples on the eastern side would include (from north to south): Tin Mine, Sugarloaf, and McMillian landslides; on the western side (from north to south): Anthony, Tom Mays, Smuggler, Flag Hill, and Crazy Cat landslides. It would seem to be reasonable to identify the gliding planes and competency failures to weakly indurated formations. These glide planes and competency failures seem to be logically largely developed in the Ordovician uppermost El Paso Group Florida Mountains Formation, the Late Devonian Percha Shale, and Late Pennsylvanian Panther Seep Formation.

The ancestral Rio Grande in the past flowed through Fillmore Pass and along the eastern side of the Franklins. This can be documented from the gravel pits and water wells in that area. Erosion along Paso del Norte, located on the southwestern side of the Franklins and east of Cerro de Cristo Rey, late in the Pleistocene captured the river by either by stream piracy or a downcutting overflow of lake developed by uplift of the Franklin chains.

Quaternary faulting was noted by Richardson (1909), who described the fault scarps of the EFMF under the heading "Bolson Faults." He stated: *"Besides the faults of relatively ancient date, which are revealed by the distribution of the strata, there are indications of later displacements involving the bolson deposits. A disconnected line of high-level benches extends along the eastern base of the Franklin Range and is well exposed west and northwest of Fort Bliss. At the southeast end of the range these benches lie at an elevation of about 3900 feet; east of the central part of the mountains they extend approximately along the 4250-foot level. They are much dissected by the many arroyos which head in the mountains and in places are inconspicuous. These benches are the upper parts of broken alluvial slopes which in places fringe the base of the range in an uneven eastward-facing scarp varying from 10 to 50 feet in height. West of the scarp the alluvial debris slopes up to the mountains, and east of the scarp the alluvium gradually descends in an even grade to the general level of the Hueco Bolson. These interrupted alluvial slopes strongly suggest Quaternary faulting that may represent renewed uplift along the old hypothetical fault which delimits the Franklin Range on the east."*

[underlining added; this is the EFMF of present usage]. That faulting in this region has actually occurred in the Quaternary is shown in a sand pit at the head of North Virginia Street.” Fig. 5 shows a typical piedmont fault scarp of the EFMF.

3. METHODS

The trench was excavated by a Cat 325 trackhoe to the width of the 1 m-wide bucket and benched on both sides. Only the inner slot was shored with hydraulic aluminum shores. For most of the hanging wall, the southern wall of the trench was cleaned by manual scraping, then a series of horizontal stringlines were attached to the trench wall, spaced 1 m apart, that served as control for the manual trench logging. However, on the footwall the northern trench wall made a better exposure so we logged that wall. The wall was logged by the manual method (McCalpin, 1996, p. 70) at a scale of 1:20. Mapping units were defined either as stratigraphic units or as soil horizons developed on stratigraphic units.

Mapping conventions: The unconsolidated map units defined on trench logs include both parent materials unaffected by soil formation (e.g., unit 25), and parent materials that have been affected by soil formation (e.g., unit 25Ck2). In the latter group the map units are soil horizons defined by changes in soil horizon properties, rather than by a change in parent material sedimentology.



Fig. 5. Photograph of the piedmont fault scarps of the East Franklin Mountains fault. View to the SW from the power line access road near the arroyo bank site. The scarps shown stretch for about 5 km south of the arroyo exposure site (out of sight to the right).

Horizons were recognized and named according to the definitions of SCS (1994) and Birkeland (1999). In each map unit abbreviation the parent material number (1=oldest) forms the first part of the unit designation and the soil horizon abbreviation (if applicable) forms the next part of the map unit designation. The final part of the map unit designation indicates whether the soil horizon is part of a buried soil (i.e., not the surface soil) and if so, the number of the buried soil, with "b1" indicating the uppermost (youngest) buried soil. Thus, the map unit designation "10Kb1" indicates that the parent material is unit 10 (sand), the soil horizon is a K horizon (strongly calcified), and the K horizon is part of the 1st buried soil counting down from the ground surface. This same naming convention is used throughout the trench logs.

4. EAST FRANKLIN MOUNTAINS FAULT STUDY SITE

Our study was limited to excavating one trench and cleaning off one arroyo exposure on a piedmont fault scarp of the EFMF. Both of our localities had been studied before, so our main contribution was to apply advanced dating techniques to the sites, as described below.

4.1 The NEHRP 1995 Study of the East Franklin Mountains Fault

Keaton and Barnes (1996) performed the only prior paleoseismic study of the EFMF. Their FY1994 NEHRP grant included fault scarp profiling, drilling, and excavation of two trenches. Their primary trench was across a ca. 8 m-high fault scarp in Jornada II (25-150 ka) alluvial fan deposits (Figs. 6, 7). A second trench was dug about 200 m north of the primary trench, in younger Isaacks Ranch alluvium (Holocene) across the projection of the fault scarp. Their trench exposed only unfaulted Isaacks Ranch alluvium, and did not reach older (Jornada II) alluvium, so no useful information was retrieved.

In addition to the two trenches, they studied a second site about 2 km north of the primary trench (Fig. 7), where an arroyo streamcut had fortuitously exposed the main EFMF. The footwall of the EFMF exposed the distinctive sandy alluvium of the Camp Rice Formation (ancestral Rio Grande alluvium), so they drilled a 45.7 m-deep auger hole on the fault hanging wall, attempting to reach the correlative top of the Camp Rice sands on the downthrown block. However, they did not reach the top of the Camp Rice Formation, indicating that the vertical separation of this datum (ca. 500 ka) across the EFMF is at least 45 m.

Most of Keaton and Barnes' (1996) seismic source characteristics for the EFMF were derived from the primary trench. However, their interpretation of the trench was based primarily on a correlation of the caliche soil profile on the footwall to a caliche soil developed on their unit 1 in the hanging wall (our unit 13Kb3, discussed later). They call this the "early Jornada II calcrete", and infer an age for it of 95-150 ka (Keaton and Barnes, 1996, p. 35). Clearly, the parent material deposits on which these two calcretes are developed are not the same unit, as recognized even by Keaton and Barnes (1996). On the footwall, the calcrete is developed on well-stratified and well-sorted gravels and sands representing clear-water or hyperconcentrated fluvial channel transport. In contrast, on the hanging wall the calcrete is developed on a fine-grained marsh deposit that has no counterpart on the footwall, and by its grain size and paleobotany, accumulated at the base of a fault scarp. The well-stratified footwall gravels are never exposed in the downthrown part of the trench, which indicates they lie at some (unknown) depth beneath the trench floor.

East Franklin Mountains Fault, Keaton and Barnes
US Geological Survey Award 1434-94-G-2389
AGRA Earth & Environmental Project E93-4149
May 10, 1996

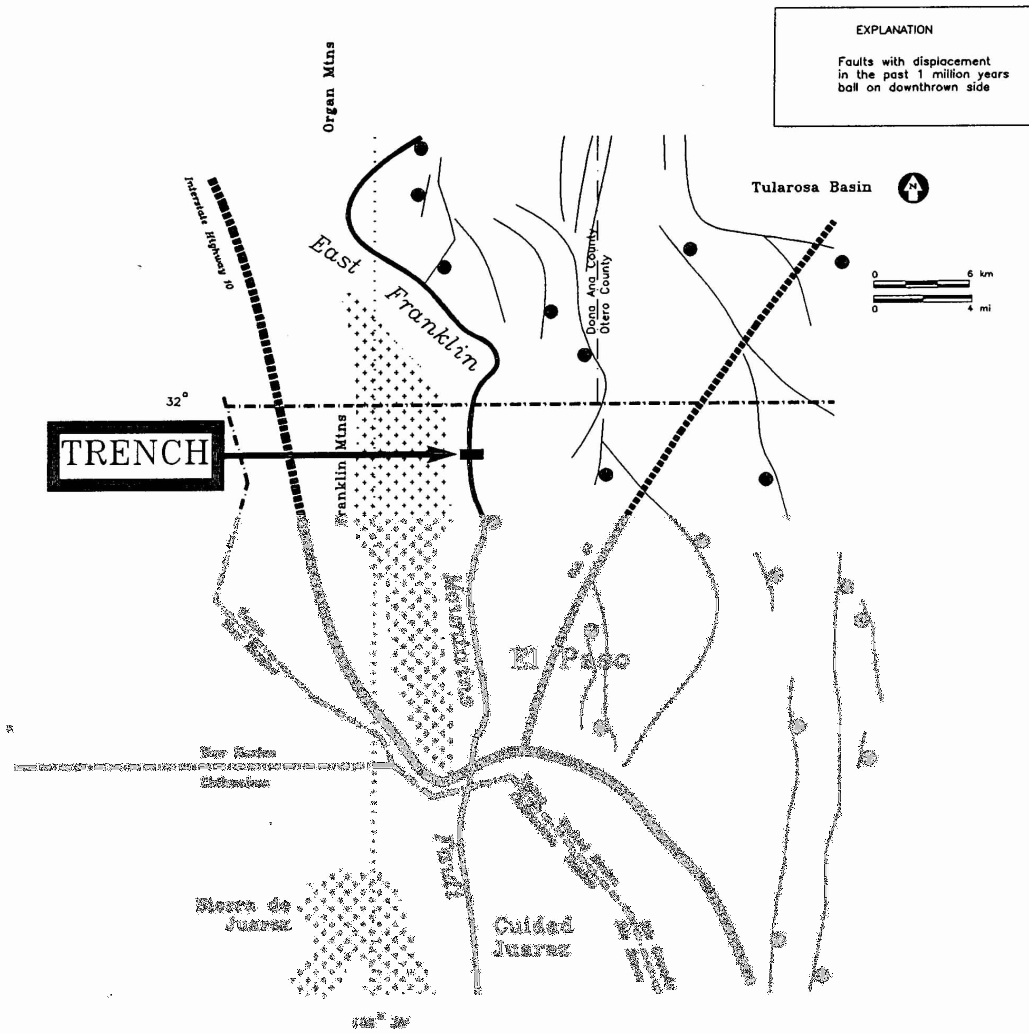


Figure 2. Generalized map of Quaternary faults in the immediate vicinity of El Paso.

Fig.6. Sketch map of the EFMF and subsidiary fault traces in the Hueco graben, from Keaton and Barnes (1996). The arrow shows their 1995 trench site, which we reexcavated in 2003.

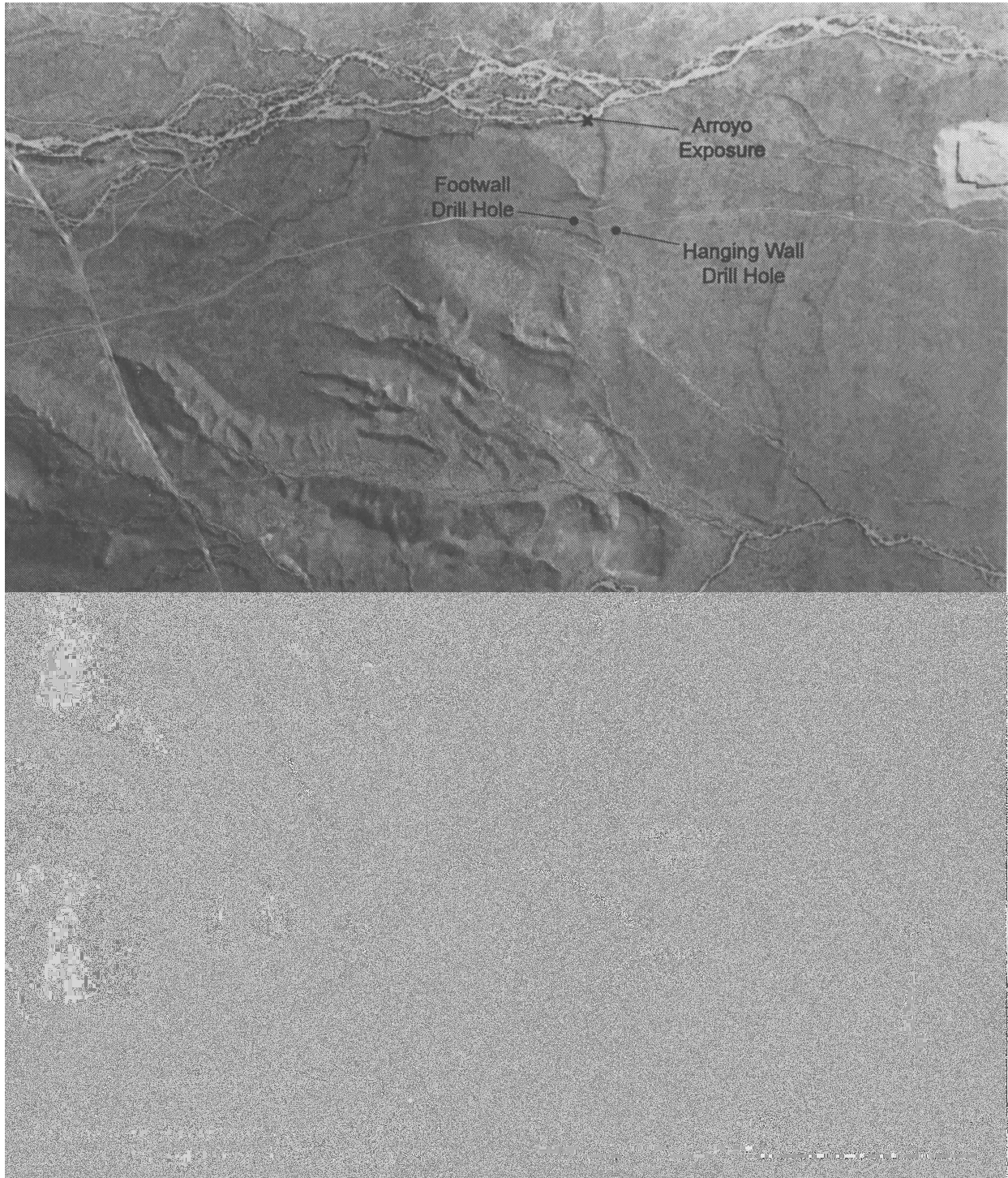


Fig. 7. Location map of trench and arroyo exposure, from Keaton and Barnes (1996).

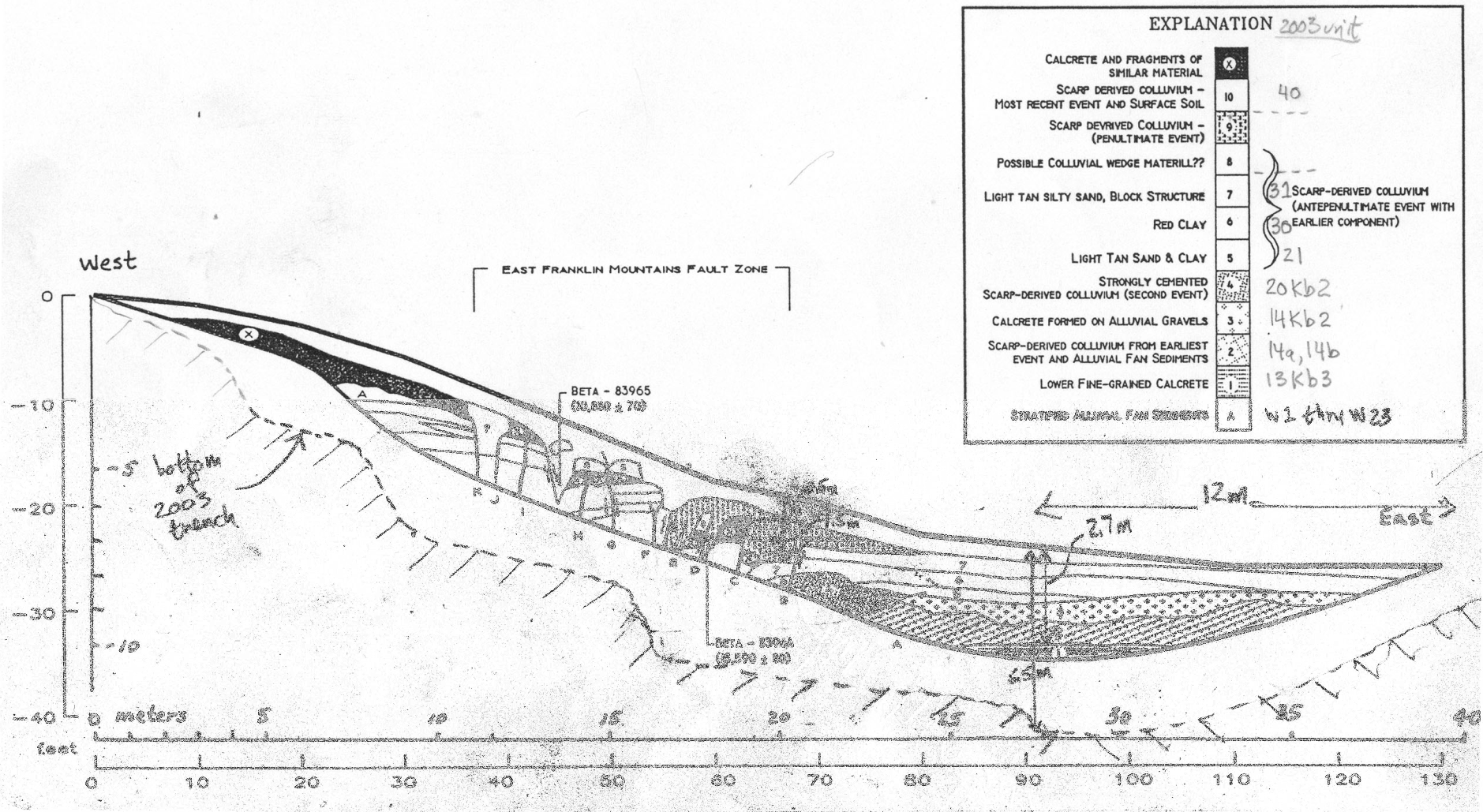


Fig. 8. Log of the north wall of the primary trench of Keaton and Barnes (1996). Dashed line below trench with diagonal ticks shows bottom of 2003 reexcavated trench. Explanation box at upper right shows correlation between 1996 trench units and 2003 trench units. The calcrete soil (black fill) as shown on this log actually represents several non-correlative soils on the footwall and hanging wall. Most of our logging was performed on the south wall, which was consistently in shadow. However, we did log the deepened north wall part of the footwall, equivalent to stations 7 m to 17 m on this log.

Based on their correlation of the two caliche soils, Keaton and Barnes (1996) concluded that by the beginning of Jornada II time (ca. 150 ka), the preexisting fault scarp here had been completely buried. Subsequently the “early Jornada II calcrete” formed a continuous sloping surface at 3 degrees across the footwall and hanging wall, sometime between 95 and 150 ka. Their palimpsestic reconstruction and slip rates were then calculated based on this assumption. As we describe later, we believe that their correlation is flawed, and that the hanging wall part of the soil is younger than 64 ka, based on luminescence dating. This means their post-Jornada Ii slip rates could be in error by a factor of nearly 2.

4.2 This Study (NEHRP 2003) of the East Franklin Mountains Fault-- Overview

Our study was designed to check Keaton and Barnes’ (1996) conclusions (particularly slip rate) by applying AMS radiocarbon and luminescence dating to their 1995 exposures. In an effort to minimize field time and expense, we reexcavated their primary trench, secondary trench, and arroyo exposure (Fig. 9). This strategy saved time for 3 reasons: (1) the stratigraphic setting of each site was already known, so all we needed to do was clean off the walls and collect the dating samples, (2) because all 3 exposures had never been backfilled, we only had to clean out the 8 years worth of weathered and sloughed material in each trench, rather than dig new trenches from scratch, and (3) no new environmental permits were required, because all 3 sites were already disturbed. To make the project more attractive to the landowner (El Paso Public Service Board), we agreed to backfill the trenches, which had stood open since 1995 (Figs. 10, 11).

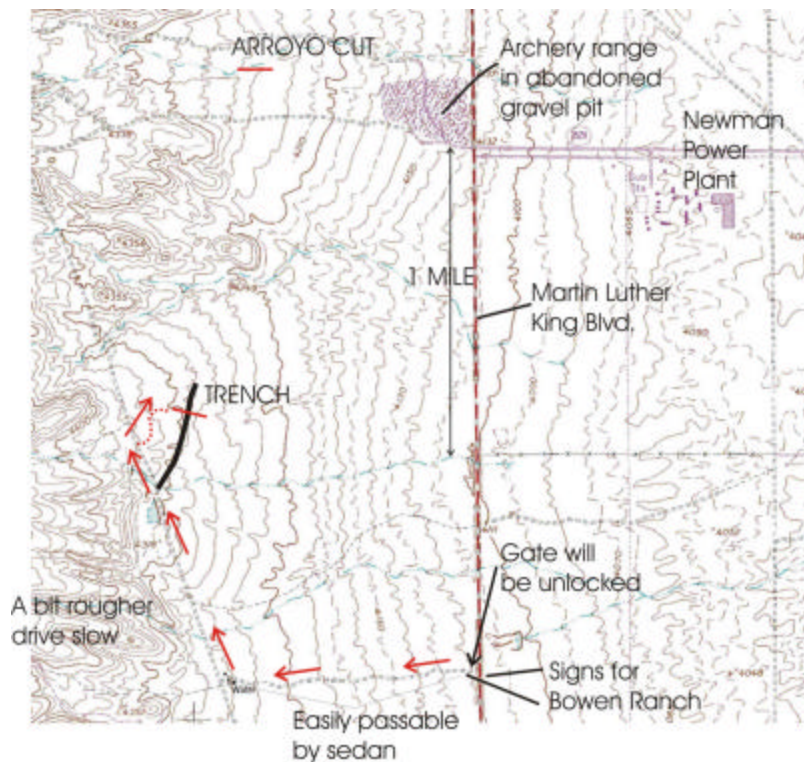


Fig. 9. Annotated map of driving directions to the 2003 trench and arroyo exposure. Base map from El Paso NE 7.5' topographic quad.



Fig. 10. Photo of the uppermost (western) part of the 1995 trench taken in March 2003, before our reexcavation. The ladder is leaning against well-stratified footwall gravels. The main fault zone is at center, in an area of the wall that has raveled back.



Fig. 11. Photo of the lower (eastern) part of the 1995 trench taken in March 2003, before our reexcavation. The main fault zone is at center, between two shrubs growing out of the top of the left trench wall.

4.3 2003 Primary Trench Site

When we wrote the NEHRP proposal in April 2002, we had anticipated only cleaning off the walls of Keaton and Barnes' (1996) trench site and collecting dating samples. However, by March 2003 we came to suspect that the entire hanging wall stratigraphic sequence was younger than the footwall stratigraphic sequence. This suggested that, as long as we had a large trackhoe at the trench, we might as well deepen the trench in the hanging wall, in hopes of exposing the correlative footwall gravels. If this was accomplished, then we could measure the true stratigraphic displacement of the Jornada II deposits, rather than base our slip rates on scarp height alone, which is merely a proxy for displacement. As a result, we ended up deepening the entire primary trench 2-3 m deeper than the 1995 trench (Fig. 8).

4.3.1 Geomorphology of Scarp

The fault scarp at the primary trench site is a relatively simple, single scarp that maintains a very uniform height across the Jornada II alluvial fan surface (Fig. 12).



Fig. 12. Telephoto view of the ca. 8 m-high fault scarp across the Jornada II alluvial fan surface at the primary trench site, which is visible at far right as a spoil pile and orange fencing. Note that the toe of the trench is not visible, due to slight backtilting or graben formation in the hanging wall. The downthrown side of the scarp has been buried by younger alluvium being transported from left (south) to right, from an arroyo off the left margin of the photo.

4.3.2 Stratigraphy

The 2003 trench exposed the same general stratigraphic framework as did the 1995 trench. The footwall sequence is composed of very similar, well-sorted, thin gravel units, and the hanging wall side is composed of heterogeneous, thicker, poorly-sorted scarp-derived colluvium, swamp and eolian deposits, debris flows, and multiple paleosols.

Footwall Stratigraphic Sequence (8 m thick): We defined 23 mappable units on the footwall (Fig. 13 and Plate 1). Our unit abbreviations begin with either W (well-sorted gravel), P (poorly-sorted gravel), or S (sand). Unit numbers increase downward. We subdivided these units so finely for 2 reasons: (1) so we could measure displacement on the subsidiary faults in the footwall, and (2) so we could recognize what part of the stratigraphic section we were in, if we did manage to expose well-stratified gravels in the deepened hanging wall part of the trench.

The 8 m-thick footwall stratigraphic sequence is amazingly well stratified for an alluvial fan environment (Fig. 14). All of the units are tabular over the exposed horizontal extent of the north wall (13 m wide) and 16 of the 22 units can be traced over this entire width (the other 6 being faulted out rather than pinching out). This consistency is remarkable because the individual depositional units are so thin, averaging between about 15-40 cm. Thirteen of the 22 units are well-sorted gravels interpreted as channel deposits of ephemeral streams. Seven of the 22 units are poorly sorted (some matrix support), interpreted as thin debris flows. Two of the 22 units are massive sands, either eolian or some type of overbank facies.

Overall, the sedimentology indicates 2 features of the environment: (1) the fan surface at the time was a sheetflood- and streamflood-dominated alluvial fan environment, rather than a debris-flow-dominated environment, and (2) the depositional environment was one of fairly steady aggradation, rather than alternating deposition and erosion at an unchanging elevation (i.e., a mainly transportational slope). For the first feature, the streamflow dominance may be partly caused by the site location about 1 mile east of the range front, so many debris flows may not make it this far out into the bolson. An alternative explanation is that streams in Jornada II time carried much more water than they do today. For the second feature, it implies that this site was on the hanging wall of the EFMF where aggradation was steady, rather than on the footwall (as it is today) where uplift would cause incision into the footwall alternating with climate-controlled aggradation. In other words, one interpretation of the sedimentology of the footwall, is that this strand of the EFMF did not exist yet when these gravels were deposited, and the active fault at the time was farther west.

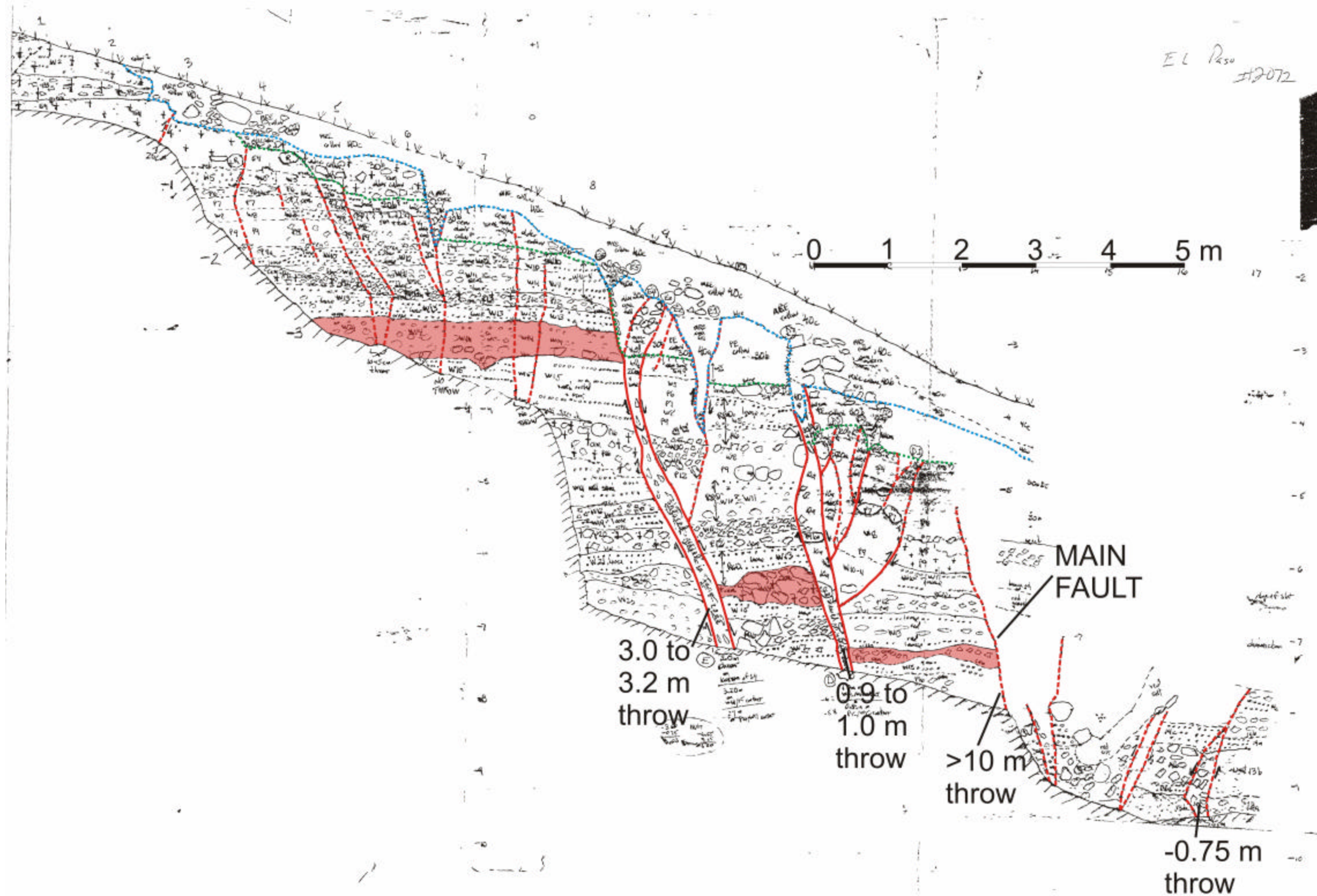


Fig. 13. Annotated field log of the footwall of the main fault, on the North Wall. Solid red lines bound well-developed fault and shear zones; dashed red lines are poorly expressed faults and fractures of little or no displacement. Blue dotted line marks base of Event Z colluvium and crack fill, green dotted line is at base of Event Y colluvium and crack fill. Unit 14 (a thin debris flow) is shaded in pink to show displacement across footwall faults E (3.0-3.2 m throw) and D (0.9-1.0 m throw).



Fig. 14. Photo of footwall on N trench wall, centered on the upper part of fault E. Red string lines define a 1-m grid. Field of view is 2 m wide and 3 m high. Note good stratification of tabular, thin gravelly and sandy beds in the footwall. No such deposits are exposed on the hanging wall side of the trench, indicating they have been faulted down-to-the-east lower than the bottom of the trench.

Hanging Wall Stratigraphic Sequence (7.5 m thick): We defined 16 mappable units on the footwall (Plate 1 and Table 2). Our unit numbers increase upward, or opposite to the numbering system used in the footwall. We subdivided these units based on gross sedimentology and degree of soil development.

The 4 youngest unit packages on the hanging wall are all scarp-derived colluviums. Unit 40 was deposited after the most recent displacement event (Event Z) and carries the modern surface soil. Unit 35 is either blocks of unit 30 that fell into a graben during Event Z, or blocks of footwall gravels (units P3, W2, W1) carrying a thinned version of the footwall relict soil. Units 30 and 31 were deposited after the penultimate displacement event (Event Y). Units 20 and 21 are colluvium (with perhaps a debris-flow component) deposited after Event X. Units 15-19 are highly deformed within the fault zone, but have no counterparts outside the fault zone, so are probably colluvial and graben-fill alluvial units deposited after before Event X, and probably represent more one Event (Event W?). Like unit 35, these units have no counterparts beyond the fault zone.

Units 10-14 are generally thick, tabular deposits of gravel ranging from well-sorted pea gravel (unit 14a) to sandy gravel (units 11, 12), to matrix-supported gravel (unit 10a). These units average about 1 m each in thickness, so are much thicker and more poorly sorted and stratified, than any of the gravel units exposed on the hanging wall. They obviously do not represent the same depositional environment as the streamflood gravels from a western source exposed in the footwall. We interpret these deposits as late Jornada II (25-65 ka) alluvium from a southern source, that was deposited up against the base of a fault scarp. However, Mike Machette (USGS-Denver) reviewed the trench and thought that all units below unit 13 (described next) could possibly correlate with the uppermost gravel units on the footwall (W1, W2, P3). One reason he thought this was that pebble imbrications in units 10, 11, and 12 appear to indicate eastward flow, perpendicular to the scarp. If these units were deposited against a preexisting scarp, they should have imbrications indicating flow parallel to the scarp.

We do not know why the imbrications are eastward in units 10-12, but in our opinion they are sedimentologically distinct from the uppermost footwall beds W1-W2-P3. Those 3 footwall beds have laterally consistent thicknesses of 50 cm, 75 cm, and 15-30 cm, respectively, or an aggregate thickness of 140-155 cm. At a depth of 155 cm below the footwall surface the distinctive sand unit S4 is encountered, which extends to a depth of 220 cm. None of the unit contacts are scoured.

In contrast, hanging wall units 12, 11, and 10 have laterally consistent thicknesses of 75, 70, and >95 cm, respectively, for an aggregate thickness of >240 cm, or 155-171% of the thickness of W1-W2-P3. Unit 11 is clearly scoured into unit 10. No sand such as S4 is encountered.

In summary, the thickness, geometry, and texture of hanging wall beds 12-11-10 just does not resemble that of footwall beds W1-W2-P3.

Table 2. Unit descriptions on the hanging wall and in the main fault zone; includes both stratigraphic units and soil horizons.

Unit No.	Sediment Package	Description
40AC 40	Slopewash and Colluvium shed after Event Z	AC HORIZON OF MODERN SOIL, DEVELOPED ON UNIT 40 Sand with minor gravel and cobbles; unstratified; loose; brown color; SCARP-DERIVED COLLUVIUM
35Bkb1 35a3 35a2 35a1	Proximal colluvium and crack fill after Event Y	Highly faulted and broken blocks of intact stratigraphy of various textures; 35a1 is very loose crack fill; 35a2 is sand overprinting with Stage III carbonate; 35a3 is sandy gravel overprinting by Stage II carbonate; 35Bkb1 is reddish sand with Stage I-II carbonate; the fact that some blocks contain B and K horizons means they predate Event Z; most likely crack-fill facies equivalent in age to units 30 and 31, but re-faulted in Event Z
31Bkb1 30Btb1	Slopewash and Colluvium shed after Event Y	Sand with very few clasts, except at basal contact (stone line); massive; red; contains some carbonate, but less than 31Bkb1; B HORIZON OF BURIED SOIL 1, DEVELOPED ON UNIT 30, SLOPEWASH AND COLLUVIUM
21Btb2 20Bkb2 20Kb2	Slopewash and Colluvium shed after Event X	Sand with very few clasts; massive; light red with rare white blebs of carbonate; very firm; B HORIZON OF BURIED SOIL 2, SLOPEWASH Gravelly sand; massive; blotchy areas of red Bt and white Stage III carbonate; weak, medium subangular blocky structure; looks like Bt horizon later engulfed by carbonate; Bk HORIZON OF BURIED SOIL 2, STONY COLLUVIUM Matrix-supported diamicton; random clast orientation; basal stone line; Stage III-IV carbonate; K HORIZON OF BURIED SOIL 2, DIAMICTON (DEBRIS FLOW?)
19 18 17 16 15	Slopewash and Colluvium shed after Event W?	Very poorly sorted diamicton, complexly faulted; contains pockets that are both clast- and matrix-supported; DEBRIS FLOW? Lens of brown sand with rare pebbles; anomalously fine-grained for this trench; massive; either loessy sag pond deposit that predates unit 20, or a block of free face stratigraphy (S4?) that fell off immediately after Event X Poorly-sorted lens of small to large pebble gravel; good imbrication to the east; contains Stage II-III carbonate; ALLUVIUM Well-sorted lens of gravel, mostly pea- and small-pebble size; well stratified; loose; contains Stage I carbonate; ALLUVIUM Cemented ledge of poorly sorted gravel; contains Stage III carbonate; similar to unit 17; COLLUVIUM OF EVENT W?
14bK1b2 14bK2b2 14bK3b2 14b 14a 13Kb3 12Kb3 12a 11 10d	Alluvium, debris flows, and sag pond sediments deposited against the scarp; long period of deposition without faulting	Stage IV K horizon; hard; laminar; developed on unit 14b, but few clasts. Stage IV K horizon developed on unit 14b gravels. Stage III K horizon developed on unit 14b gravels; spotty areas of carbonate overprinting Gravel; pea size with cobbles; contains weakly stratified lenses; STREAM ALLUVIUM Sand and gravel; pea size; well stratified; loose; STREAM CHANNEL ALLUVIUM Silty sand to sandy silt; no clasts; strong overprint of Stage IV pedogenic carbonate; SAG POND SILT Gravelly silt; matrix-supported; unstratified; max. clast size 22 cm; clasts round to subround, various lithologies; strong pedogenic carbonate overprint; DEBRIS FLOW Sandy gravel; clast supported; forms a pod-shaped unit at the east end of trench; STREAM ALLUVIUM Sandy gravel; clast supported; max. clast size 35 cm., avg. clasts 3 cm; well stratified; STREAM ALLUVIUM Sandy gravel; max. clast size 60 cm, avg. clasts 4 cm; red; weakly stratified; STREAM

	ALLUVIUM
10c	Transitional between units 10d and 10b
10b	Fracture-bounded block containing both matrix-supported debris flow deposits and clast-supported, loose, pea and small pebble gravel; STREAM ALLUVIUM
10a	Bouldery silt; unstratified; very poorly sorted, except for medial bed of golfball-size gravel' matrix-supported; DEBRIS FLOW

Our interpretation of units 10-14 as inter-faulting alluvium, younger than the footwall sequence, is supported by the existence of unit 13, a massive silty sand deposit. This deposit is unlike any other deposit exposed in the trench, because it contains no clasts and has a greenish, reduced appearance. The silt also contains many tiny angular void spaces that give it a vesicular character. The lack of clasts and reduced color suggested that unit 13 might be a marsh (cienea) deposit that accumulated in swampy conditions at the toe of a fault scarp. At present, even the toe of the fault scarp is in the Lower Sonoran life zone, as defined by Merriam and Steineger (1890): (“**Lower Sonoran Life Zone.** This vegetation of this life zone corresponds with the hot deserts of the southwestern United States and northwest Mexico (the Mojave, Sonoran, and Chihuahuan deserts). Creosotebush (*Larrea tridentata*) and other desert shrubs and succulents occur at elevations from 100 ft to 3,500-4,000 ft above sea level. Total annual precipitation averages 10 inches or less”).

To confirm this hypothesis, we contracted Paleo Research Institute in Golden, CO to perform a pollen analysis (see Appendix 4 for whole report). Their conclusions state “*The pollen assemblage noted in the sample suggests a bosque plant community rather than a cienega. These communities are typically dense stands of mesquite and acacia trees with oaks well represented in the higher elevations. Given that this soil was being developed ~30,000 years ago during a period of colder climate, a mixed oak/mesquite bosque would not be unexpected if moisture were available. The presence of mints and cattails indicates that not only was subsurface water available, but that there was open water or perennially marshy conditions in the area*” (Varney, 2004). The pollen assemblage is thus more representative of the Upper Sonoran life zone (“**Upper Sonoran Life Zone.** A number of communities are characteristic of this zone that ranges from 3,500-4,000 ft to about 7,000 ft in elevation. These include a woodlands of evergreen oaks (*Quercus* spp.), pinyon pine (*Pinus cembroides*), and/or juniper (*Juniperus* spp.); the Arizona chaparral of leathery-leaved scrub oaks (e.g., *Quercus emoryi*), manzanita (*Arctostaphylos* spp.), buckthorn (*Rhamnus* spp.) and mountain mahogany (*Cercocarpus* spp.); grassland; and Great Basin desertscrub with its dominant sagebrush (*Artemisia tridentata*). Total annual precipitation varies from 8 to slightly more than 20 inches”).

At the time the report was written, the only age control for unit 13Kb3 was a radiocarbon age on soil carbonate, which indicated an approximate age of 30 ka. Subsequently, we received the IRSL age of this unit from Desert Research Institute as 64.1±5.7 ka. That age, despite being twice as old as the radiocarbon age, also (coincidentally) corresponds to a cool period (Stage 4) in the marine oxygen isotope record (Fig. 13).

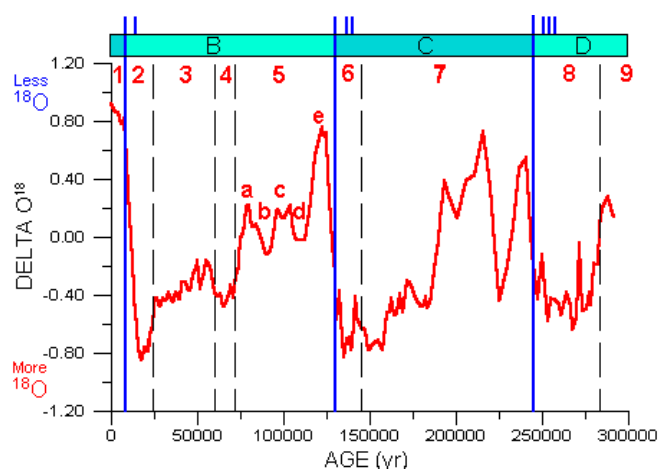


Fig. 15. Plot of delta O¹⁸ in marine sediments, from Imbrie et al. (1992). The luminescence age of unit 13 (64,000 years) places it in Marine Oxygen Isotope Stage 4, a cool period.

4.3.3 Soils

The soil profiles developed in the primary trench follow the same pattern as those on normal fault scarps studied elsewhere (McCalpin and Berry, 1996; McCalpin, 1996b). On the footwall side of the scarp there is only a single surface soil, which is best developed above the crest of the scarp (Av/Bk/K1/K2/Ck/Cox) and becomes progressively thinner on the upper scarp face, until it is truncated at the fault zone. This soil is a relict soil (also the surface soil), defined as the soil that has continuously developed on the upthrown fault block, subsequent to its abandonment as an active geomorphic (depositional) surface. The early Jornada II alluvial fan surface was abandoned as a depositional surface as soon as the ephemeral streams draining the piedmont began to incise into it. Such incision may have been caused by either tectonic uplift along the fault scarp, or by climate change. There are no buried soils in the footwall, so that stratigraphic sequence appears to be one of nearly uninterrupted deposition.

On the hanging wall there are 4 soils, the surface soil and 3 buried soils. The surface soil 40A/40 or 40AC) is developed on unit 40, the colluvium shed after Event Z. The first buried soil (either 30Btb1, or 31Bkb1/30Btb1) is developed on units 30 and 31, the colluvium shed after Event Y. Beneath the toe of the scarp, the soil contains very little carbonate (30Btb1). Beneath the lower scarp face, carbonate related to the surface soil (40A/C) has infiltrated through the entire thickness of unit 40 and then precipitated in the upper part of unit 31. This explains the anomalous situation of having a calcareous 31Bk horizon atop a noncalcareous 30Bt horizon; the calcite is coming from an overlying soil.

The second buried soil (21Bkb2/20Bkb2/20Kb2) is a strong calcareous soil developed on the colluvium shed after Event X. The strength of carbonate development indicates that either: (1) soil b2 had more time to develop than did soil b1, or (2) soil b2 formed under a more arid climate regime than did soil b1), or (3) both.

The third buried soil is a strong carbonate soil (13Kb3/12Kb3) developed in the sag pond silt of unit 13 and in the underlying coarse fluvial gravels of unit 12. From their sedimentology and geometry it is clear that neither of these units is scarp-derived colluvium, nor are the units beneath them (units 11,

10). Mike Machette (2003, pers. comm.) thought that some of the abundant carbonate in the sag pond unit 13 may have accumulated contemporaneous with sediment accumulation in a spring (cienega) setting, rather than being post-depositional pedogenic carbonate.

We did not define soil horizons *per se* in the fault-bounded block (faults A, B, and C) that contains units 15-19, even though units 15 and 19 both contain carbonate. The carbonate in those units appeared to conform so closely to the textural changes between units, that we were not convinced it was all pedogenic.

Our conceptual model of soil formation on a normal fault scarp is based on 3 principles: (1) the equivalence of total soil development time on the footwall and hanging wall, (2) continuous soil formation of the relict footwall soil versus episodic deposition and soil formation on the hanging wall, and (3) higher soil development rates on the hanging wall, due to greater moisture availability and redeposition of eroded footwall soil components (clay and carbonate) into hanging wall parent materials. In this model, we assume that the scarp was mantled by a soil profile during every inter-faulting hiatus. Thus, each hanging-wall soil partially correlates with the relict footwall soil, which has been developing continuously during faulting. Each hanging wall soil was physically connected at one time to the relict soil, until it was truncated by the next faulting event.

Based on this model, we would not state that any one hanging wall soil correlated with the footwall soil, as did Keaton and Barnes (1996). Instead, all 4 hanging wall soils are partially time-equivalent to the footwall soil. The cumulative soil development time of all hanging wall soils equals that of the relict footwall soil. In the primary trench, we believe that there are additional, unexposed hanging-wall soils beneath the trench floor, and that our sequence of 4 hanging-wall soils is only a partial record of all the hanging-wall soils that have formed since the relict footwall soil began forming (120-150 ka). For example, the oldest of our 4 hanging-wall soils dates at only 64 ka, or about half the age of the footwall relict soil. If we had been able to deepen the trench another (say) 5 m, we anticipate that more hanging-wall soils in the age range 64-150 ka would have been exposed.

We sampled all the paleosols so that, if all other attempts at dating failed, we could calculate the weight percent of carbonate in all soils (footwall and hanging wall), and then estimate soil age based on total carbonate (grams) and an assumed rate of carbonate accumulation (grams/kyr). Fortunately, the luminescence ages came out generally in correct stratigraphic order and comparable to the estimated ages of Jornada II deposits, so we have not processed those samples, and they remain in storage at GEO-HAZ.

4.3.4 Structure

The EFMF exposed in the trench is composed of 5 normal faults, lettered A through E (from east to west) on Plate 1 and Fig. 13. The main fault is fault C, which dips about 80°E and flares upward into a tension fissure and then into a 2 m-wide graben at the surface (Fig. 16). Due to the complexity of the fault near the surface, we identified 5 fault planes (C1 through C5) that merge downward into the two bounding faults of a 30 cm-wide shear zone at the bottom of the trench. Vertical displacement (throw) on fault C is >7.5 m, which is the vertical distance between the top of the reconstructed stratigraphic sequence on the footwall, and the bottom of the trench on the hanging wall (no correlative

units exist on the hanging wall). Fault C displaces all hanging wall units except for unit 40 (colluvium of Event Z).

Faults D and E are down-to-the-east normal faults in the footwall, the former 2 m into the footwall and the latter 3.5 m into the footwall. Fault D dips about 75-80E and is marked by a 15-25 cm-wide shear zone on both trench walls (Fig. 13). In both walls one or more west-dipping reverse faults splay off from fault D within 1 m of the trench floor. These faults have minor displacement (60 cm on one strand on the south wall, perhaps a similar amount on two strands on the north wall). Total down-to-the-east throw on the main part of fault D (below the reverse splays) is 0.95-1.00 m on the north wall and 0.70-1.00 m on the south wall (varies irregularly depending on the datum measured). Fault D displaces all units except unit 40.

Fault E is also a down-to-the-east normal fault, but has a significantly wider shear zone (25-30 cm) with well-developed fault-parallel clast fabric, and more displacement (2.7-3.2 m on the north wall, 3.1 m on the south wall). Fault E displaces all units except unit 40.

On the hanging wall there are 2 faults, A and B (Plate 1). Fault B is closest to the main fault C (about 0.75 m away), but is rather anomalous in that it is vertical, undulatory, and only has clear displacement in units 13 and 14 (about 20 cm down-to-the-east). The fault appears to extend upward into units 15-19 and to shear them, but without effecting much measurable vertical displacement. Therefore, this fault did not experience measurable displacement in Events Z, Y, or X.

Fault A lies in the hanging wall about 1.5 m E of the main fault, and is a normal fault that dips west (antithetic fault). The fault displaces the bottom of unit 20Kb2 but does not extend through the unit into unit 21Btb2. Therefore, it experienced its last major movement in Event X, although it may have had a small amount of down-to-the east displacement in Event Y.

The odd thing about fault A is that it displaces the bottom of unit 20 down-to-the-east, but displaces underlying units 13 and 14 down-to-the-west. This relationship requires that fault A was originally a down-to-the-west antithetic fault prior to Event X, and defined a graben with fault C, but by Event Y had become a down-to-the-east fault.

The overall pattern of faults and their upward terminations suggest that faulting is advancing into the footwall with time. Faults A and B have not experienced major movement since Event X. Prior to that, they formed a graben that filled with units 15-19. Beginning with Event X, these faults have become abandoned and displacement has transferred to faults C, D, and E. The same pattern was observed by McCalpin (in press) on the Calabacillas fault near Albuquerque, New Mexico.



Fig. 16. Photo of the upper (graben) part of the main fault zone (fault C) on the south wall. Orange lines show fault traces C1-C5 shown on Plate 1.

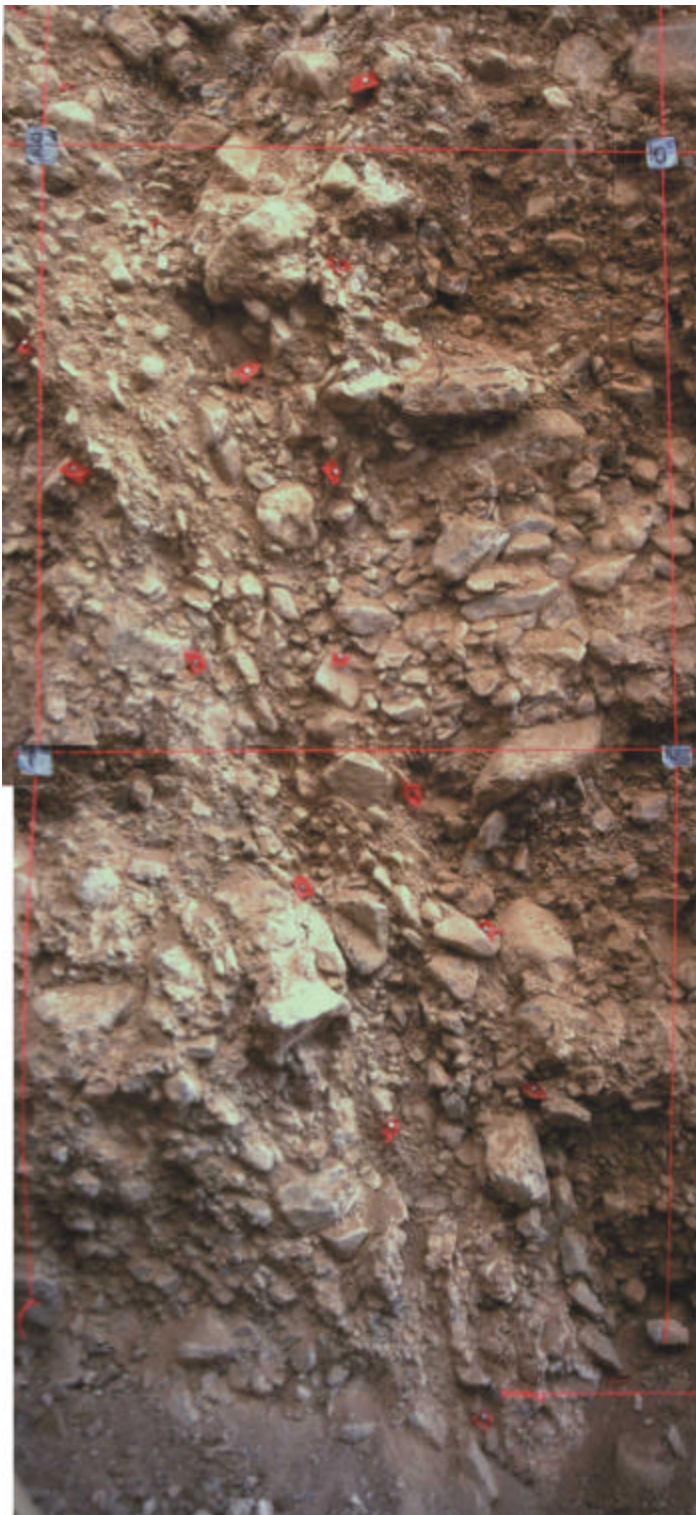


Fig. 17. Photo of the lower 2 m of fault E (between red flagging on wall) on the north trench wall (compare to Fig. 13). The zone of sheared footwall gravels is about 25 cm wide. This fault has a net throw of 3.0-3.2 m.

4.3.5 Geochronology

Due to the aridity of the site, organic carbon was extremely rare in the trench walls. Those small pieces observed were usually suspected to be decayed roots, and to be considerably younger than the host strata. Following the lead of Keaton and Barnes (1996), we collected 15 samples of inorganic CaCO₃ in hopes that the apparent radiocarbon ages of the carbonate would provide at least rudimentary stratigraphic age control. Admittedly, this was a desperation move, because radiocarbon ages of carbonate paleosols are difficult to interpret (Chen and Polach, 1986; Stadelman, 1994). However, some authors (e.g., Cerveney et al., 2006) state that “*radiocarbon dating of pedogenic carbonate generally carries the assumption that pedogenic radiocarbon can still be used as a chronometric tool with success if one is cautious (Amundson et al., 1994; Wang et al., 1994; Deutz et al., 2001). Wang et al. (1996) concluded that ¹⁴C dating of pedogenic carbonate laminations is a useful additional tool in Quaternary studies*” (p. 379). However, laminated carbonate was rare in our trench, so most of our samples were composed of massive, non-laminar, relatively soft, silty carbonate matrix. We instructed the laboratory to separate any sand or gravel from the silt-sized carbonate matrix (but no other sample pretreatments), and then to date the matrix.

Data on the 15 radiocarbon samples are listed in Table 1. We decided to date only 3 of these samples in this manner by an initial round of dating. After we received the results, we would compare them to the ages of the less abundant luminescence samples. If the ¹⁴C dates corresponded to the luminescence dates, we would then have more confidence in them, and could date the full suite of 15 samples collected. If the ¹⁴C dates on soil carbonate consistently failed to correspond to the IRSL ages, then we would not proceed to a 2nd round of ¹⁴C dating. The latter situation actually occurred, as described later in this section.

Table 3. Summary of 15 radiocarbon samples collected and 3 dated. Dating by Beta Analytic, Miami, FL. Details are given in Appendix 3.

Sample	Unit	material	Lab. No.	Radiocarbon Age (14C yr BP)	Calibrated Age (cal yr BP)	Significance
EPC1-a	Base of 40	Very black nodules in very soft pocket, but not a root (film can)				Close MIN age on Event Z
EPC2-a	Base of 40	Smaller, lighter-colored chunk; not in a soft pocket, so probably not in a burrow (film can)				Close MIN age on Event Z
EPC3-a	14b	Charcoal (decayed root?)				Predates latest 4-5 events
EPC2	10 (graben)	Calcite cement in well-sorted gravel; dated silt fraction	β-186911	29,520±260; AMS date	N/A	Oldest bed on hanging wall

		only				
EPC3	12Kb3	Middle of debris flow; calcareous matrix				
EPC4	13Kb3	K horizon developed on sag pond silt				
EPC5	20Kb2	Base of diamicton unit				
EPC6	20Kb2	Base of Kb2 soil in diamicton; carbonate silt	β -186912	23,520±160; conventional date	N/A	
EPC7	S22	Very hard silt, Stage IV CaCO ₃				Oldest bed on footwall (sag pond silt?)
EPC8	31Bkb1	Carbonate matrix	β -186913	9,720±70; conventional date	11,120 to 11,200	
EPC9	S4?	Top of S4? Equivalent soil (K horizon)				
EPC10	21Kb2	Top of unit				
EPC11	40A	Base of modern A horizon				MIN age of Event Z
EPC12	35	In graben				
EPC13	40	base				Close MIN age on Event Z

The oldest bed on the hanging wall (unit 10) yielded a radiocarbon age of $29,520 \pm 260$ ¹⁴C yr BP, while overlying unit 20Kb2 yielded a radiocarbon age of $23,520 \pm 160$ ¹⁴ C yr BP. Although these ages are in correct stratigraphic order, they are both much younger than luminescence ages from the same strata. Unit 31Bkb1 (the buried soil developed on scarp-derived colluvium of Event Y) yielded a calibrated age of 11,120 to 11,200 cal yr BP.

We mainly relied on infrared-stimulated luminescence dates for age control, dating the fine silt fraction. The drawback to this fine-grained IRSL technique was that most units in the trench were too coarse-grained (gravel, sand) for the IRSL method. Only a few units had a significant component of inorganic silt, and in some of those units (e.g., debris flows like unit 20), the silt was not thought to have undergone complete luminescence zeroing. As a result, we only were able to collect 5 luminescence samples and only dated 4 of those.

The stratigraphically lowest luminescence sample came from unit 13Kb3, a silty sag-pond type deposit [ciénega (?) deposit] near the bottom of the exposed hanging wall stratigraphic sequence. This unit yielded a luminescence age of 64.1 ± 5.7 ka (Table 4). In almost all settings, luminescence ages should be treated as maximum ages, because any incomplete zeroing will lead to inherited luminescence

Table 4. Summary of multi-aliquot infrared-stimulated luminescence measurements on the fine silt fraction; detection at 420 nm; errors are one sigma. Dating by Glenn Berger at Desert Research Institute, Reno, NV.

Sample	Unit	material	Depth below ground surface	Dose Rate (Gy/ka)	Equivalent Dose (Gy)	Age (ka)	Significance
EPTL-1	13Kb3	Sag-pond silt impregnated with calcium carbonate	4.0 m	3.84±0.14	246±20	64.1±5.7	Pre-dates latest 4-5 faulting events
EPTL-2	30Btb1	Distal colluvium/ slopewash	1.0 m	5.59±0.21	231±22	41.3±4.2	Base of Y wedge; MIN DATE on Event Y
EPTL-3	21Btbk	“	1.35 m	4.61±0.14	175±17	38.0±3.9	Top of X wedge; MAX DATE on Event X
EPTL-4	Unit 31 (graben)	Chunk of soil downfaulted in Event Z	2.2 m	5.30±0.27	94±11	17.7±2.3	MAX DATE on Event Z
EPYL-5	S4 equivalent	Carbonate-impregnated sand					Predates abandonment of footwall alluvial fan surface

and a luminescence greater than true age, whereas the reverse is not possible (sediments cannot be “over-zeroed”). The 64 ka age is considerably younger than the inferred 120-150 ka age of the early Jornada II gravels that underlie the footwall, and reinforces the conclusion that the entire hanging-wall sequence exposed in the trench is less than half the age of the footwall sequence.

The next highest samples are a pair on either side of the contact between units 30Btb1 (colluvium from the penultimate event, Event Y) and 21Btbk (colluvium from the antepenultimate event, Event X). These samples are weakly stratigraphically reversed, with the upper sample yielding an age of 41.3 ± 4.2 ka and the lower sample yielding an age of 38.0 ± 3.9 ka (Table 3). However, these ages overlap by >50% at 1 sigma.

The youngest luminescence sample came from unit 31, a block of soil that was downfaulted into the main fault graben during the most recent event (Event Z). Although that sample also yielded an age in correct stratigraphic order (17.7 ± 2.3 ka), it is quite a bit younger than the sample that came from subjacent unit 30 outside the graben (41.3 ± 4.2 ka), and there are no unconformities between those two units as logged. Perhaps the sample was partially re-zeroed during deposition into the graben at around 10 ka, which would explain why its age comes out intermediate between that of Event Y (ca. 40 ka) and Event Z (ca. 10 ka).

4.4 Interpretation of Primary Trench Site

4.4.1 Number of Paleoseismic Events Interpreted

The primary trench exposes evidence for 3 unambiguous paleoseismic events. These younger events (Z, Y, and X) are each represented by stratigraphically-superposed, scarp-derived colluvial wedges. In addition, some fault traces that displace a lower colluvium are truncated at the bottom of the overlying colluvium, indicating that these 3 stacked colluvia are not merely the results of climatic fluctuations.

Graben fill atop the main fault on the south wall contains some material (unit 35) of unknown origin between the unambiguous colluvium from Events Z and Y. This material exists only in the graben, and clearly predates unit 40, because it contains well-developed soil horizons (Bkb and K horizons). Unit 35 could have one of two origins. The first is blocks of free face (footwall) material that fell into the graben immediately after Event Z (i.e., proximal debris-facies colluvium). The free face here would have to have been composed of units overlying unit S4, that is, units P3, W2, and P1 (cf. Fig. 14). Those units do contain gravel and sand that somewhat resemble the blocks within unit 35.

The second possible origin is proximal colluvium deposited in the graben after Event Y, and then re-ruptured and broken during Event Z. However, such colluvium would also have been derived from footwall units P3, W2, and P1, so it is difficult to differentiate between this origin and the first origin proposed. Notably, this interpretation requires that the large tension fissure-graben along the main fault was formed at least as early as Event Y, and there is independent evidence that is true (more non-correlative fissure fill deposits beneath unit 35). Regardless of which origin is correct, these noncorrelative beds can be explained with postulated an additional displacement event between Events Y and Z.

In contrast, non-correlative units 15-19 are harder to explain without invoking at least one event older than Event X. These 5 units exist only in the block bounded by faults A and C. They contain

displacement on faults (e.g., fault B) that does not affect younger units such as unit 20. The displacement on fault B could arguably have occurred during Event X, after which the post-Event X colluvium (unit 20) was deposited over the fault trace. However, there are two lines of evidence supporting pre-Event-X faulting. First, between faults A and B is a short, west-dipping shear zone that deforms 15-17, but not 18. In other words, the structure does out within the unit 15-19 package, and does not even reach the base of unit 20 (the post-Event-X colluvium). Given this relationship, it seems imperative that the movement on this fault predates Event X. Second, the sense of displacement across fault A changes updip. At the top of the fault, the displacement of the bottom of unit 20 is 50 cm down-to-the-east (synthetic movement). In contrast, across all the remainder of the fault, the sense of displacement of units 12, 13, and 14 is down-to-the-west (antithetic movement). As a result, units 15-19 comprise a 2-2.5 m-thick stratigraphic section between faults A and C, but east of fault A, unit 20 lies directly atop unit 14, and that entire stratigraphic section is missing.

One way to explain how units 15-19 could exist between faults A and C but not beyond them, is to postulate that faults A and C defined a graben prior to Event X. Units 15-19 would have accumulated only in this graben at the base of the paleo-fault scarp, as blocks of material fallen from a free face, or perhaps a mixture of blocks, colluvium, and inter-faulting alluvium. In this scenario, units 15-19 are an older and larger counterpart of unit 35. Such a scenario also requires that faults A and C defined a graben prior to Event X.

The critical question is, how many faulting events older than Event X do we have evidence for? The basal unit of the sequence (unit 15) looks like an eastward-tapering lens of poorly-sorted scarp-derived colluvium, and it lies directly upon unit 14b, which is clearly a tabular alluvium that can be traced to the eastern end of the trench. Thus, unit 15 has the stratigraphic position, shape, and sedimentology to be a scarp-derived colluvial wedge.

Units above unit 15 look more like alluvium (unit 16), debris flows (units 17, 19) and sag pond deposits (unit 18) than scarp-derived colluvium. For example, unit 16 is well-sorted gravel that maintains a constant thickness laterally, so does not resemble a colluvial wedge. Unit 17 is a matrix-supported diamicton, but is much thinner than the scarp-derived colluviums shed after Events X, Y, and Z. Unit 18 is a light reddish sand with few subrounded gravel clasts, and looks more like a pond or swale deposit than scarp-derived colluvium.

In summary, structural relationships on the trench wall demand at least 3 and probably 4 displacement events subsequent to deposition of hanging wall unit 14. We did not date unit 14, but subjacent unit 13 yielded an IRSL age of 64.1 ± 5.7 ka.

4.4.2 Displacement Per Event

The displacement in each event on each fault can be estimated in several ways. First, if a scarp-derived colluvium exists on both sides of the fault, then the vertical displacement of that colluvium can be unambiguously attributed to later events. For example, the Event Y colluvium has been displaced across footwall faults D and E on the north wall, and this displacement could only have occurred during Event Z. Second, if the cumulative displacement is known, and the displacement in all but one of the events is known, displacement in the unknown event must be the residual between the displacement in the known events and the cumulative displacement. Third, if there are no correlative units across the fault, but scarp-derived colluvium exists on one side, the minimum displacement of that colluvium can be measured, and that is a minimum estimate for the throw on all events younger than the colluvium. Fourth,

if all else fails, one can use Ostenaar's Rule of Thumb, which states that the displacement during an event is roughly twice the thickness of the scarp-derived colluvium deposited after that event.

We employed all these methods to estimate the displacement in Events W, X, Y, and Z on each of the 5 faults in the trench (Table 5). The only drawback is that, for fault C (the main fault), we have no correlative units across the fault (except for unit 40, which is unfaulted), so can only make a minimum estimate of the cumulative throw.

Table 5. Estimated displacements per event in the EFMF primary trench.

Event	Age (ka)	Displacement (m)					
		Fault A	Fault B	Fault C	Fault D	Fault E	TOTAL
Z	13-17 ka	0	0	1.2 [§]	0.7*	1.1*	3.0
Y	38-41 ka	+0.3	0	2.0 [§]	0.15 [^]	2.0 [#]	4.45
X	41-64 ka	-0.4	0?	3.2 [§]	0.15 [^]	0	2.95
W	<64 ka	-0.6	0.3	>1.1?	0	0	>0.8
	TOTAL	-0.7	0.3	>7.5	1.0	3.1	>11.2

* based on displacement of the bottom of the PE (penultimate event) colluvium; see Fig. 13.

there are only two ages of colluvium on fault E, so cumulative displacement is partitioned between events Z and Y

[^] there are 3 colluviums on Fault D, so the pre-Event-Z displacement residual was partitioned equally between Events Y and X

[§] estimated as twice the thickness of the post-Event colluvium, using Ostenaar's Rule of Thumb

? residual between the cumulative total and the total of Events X, Y, and Z

The better-constrained events X, Y, and Z have estimated displacements of 3.0, 4.45, and 2.95 m, respectively. By comparison, Keaton and Barnes (1996) estimated a "characteristic" throw of 2.36 m in event Z, by correlating alluvial fan gravels across fault E. By visually matching strata across the fault, they also reconstructed "non-characteristic throws" of 2.70, 2.22, and 2.15 m for events Z, Y, and X, respectively. All these throws assumed that the strong calcareous soil developed on units 12 and 13 (our buried soil 3) was contiguous with the Stage IV footwall relict soil in "early Jornada II time" (120-150 ka). In contrast, we do not make that assumption.

The small displacement estimated for event W (>0.8 m) is a minimum value, because we only have a minimum estimate of the cumulative displacement on fault C. For example, if the true cumulative displacement on fault C was 9.5 m rather than >7.5 m, then the displacement in event W would increase by 2 m to 2.8 m.

4.4.3 Recurrence Interval Between Paleearthquakes

As can be seen in Table 5, the age control on each individual paleoearthquake is rather poorly constrained. Given this fact, the best approach is to calculate an average recurrence between the past 4 events. The 4-event sequence spans 3 recurrence intervals. These 3 intervals post-date unit 13

(64.1 ± 5.7 ka) and end with event Z at 13-17 ka. Therefore, the 3 intervals span 41.4 to 56.8 ka, and have an average length of 13.8-18.9 ka (mean 16.4 ka).

4.4.4 Slip Rates

Theoretically, we could compute a closed-cycle slip rate for each of the 3 complete seismic cycles (W to X, X to Y, Y to Z) interpreted for this trench. However, such single-cycle estimates would have high uncertainty, because of the poor age control for each event, and the assumptions made when estimating displacements per event (Table 5, footnotes).

A more robust slip rate estimate can be made by aggregating all the displacement (>11.2 m) of the latest 4 events, all of which has occurred subsequent to unit 13 (64.1 ± 5.7 ka). This slip rate includes the 3 complete cycles referred to above, plus parts of 2 incomplete cycles (pre-event-W, post-event-X), and yields a mean minimum slip rate of 0.175 mm yr (0.16 - 0.19 mm/yr given age uncertainties). That value is plotted graphically on Fig. 18. If we wish to ignore the partial seismic cycles, then over the latest 3 closed seismic cycles the fault has released about 10.4 m of slip over a period of 41.4-56.8 ka, for an average slip rate of 0.18-0.25 mm/yr.

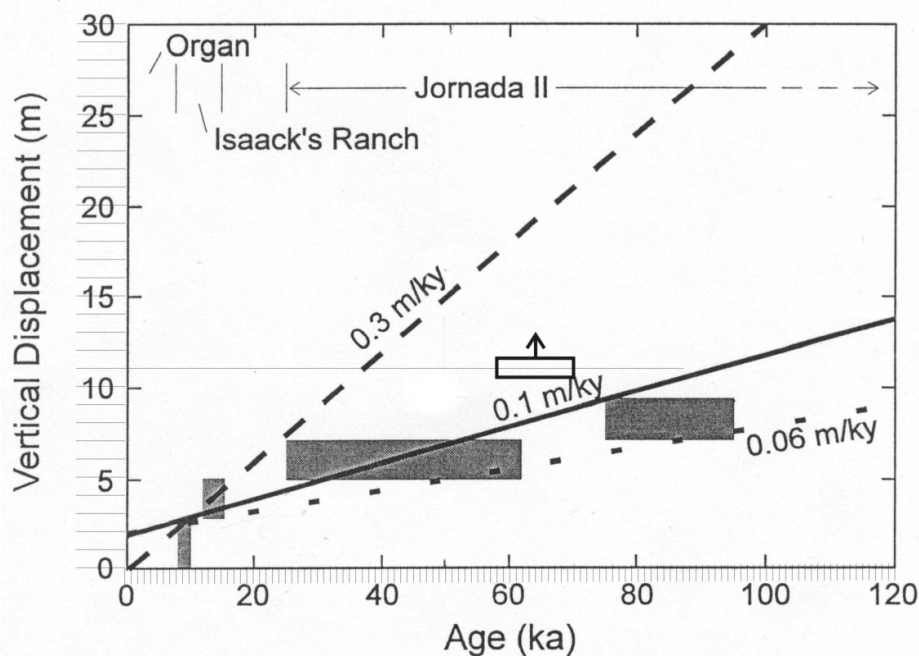


Fig. 18. Vertical displacement as a function of deposit age, adapted from Keaton and Barnes (1996). The minimum post-unit 13 (64.1 ± 5.7 ka), mixed-cycle slip rate is defined its >11.2 m displacement (hollow box with arrow at center), yielding minimum slip rates of 0.16-0.175-0.19 mm/yr.

The slip rates cited above range from about 0.16 to 0.25 mm/yr, and are all higher than Keaton and Barnes' (1996) slip rate of 0.10 mm/yr. Their slip rate was based on an inferred age of ca. 95 ka for buried soil 3 on the hanging wall, which they thought was displaced 9.2 m. Our data show that this soil is only 64 ka and is displaced more than 11.2 m.

However, there are two reason why the rates 0.16-0.25 mm/yr measured in the trench could be overestimates of the true slip rate at this site. First, the far-field scarp profile suggests there has been an

unknown amount of backtilting toward the fault, which would make displacements measured at the fault larger than the (true) net vertical displacement across the entire deformation zone. In addition, it is not clear that the scarp was completely buried by hanging wall aggradation prior to Event W. In that case, the net displacement of unit 13 is less than 11.2 m, because it was not at the same elevation as the top of the footwall prior to Event W. Because of these caveats, we recommend a slip rate of ca. 0.18 mm/yr be used for this site.

4.5 Arroyo Exposure Site

We revisited the arroyo exposure described by Keaton and Barnes (1996), and used a backhoe to deepen the exposure of the fault zone (Fig. 19).



Fig. 19. Photo of the arroyo exposure after deepening along the fault zone (visible at center); view is to the south. Well-stratified sands on the footwall (right) are Camp Rice Formation. Heavily cemented gravels at left are the colluvial wedge sequence.

4.5.1 Geomorphology

The fault scarp at the arroyo exposure is only about 5-6 m high, and separates Jornada II fan gravels on the footwall from younger alluvial fan gravels on the hanging wall. Clearly the footwall here has been periodically buried by deposits from the arroyo, and this pattern has persisted for a long period of geologic time. For example, on the footwall the sands of the Camp Rice Formation lie only about 2 m below the ground surface, but on the hanging wall the top of the Camp Rice Formation is more than 45 m below the ground surface (Keaton and Barnes, 1996). Stated another way, there is 43 m more Jornada and post-Jornada alluvium on the downthrown block than on the upthrown block.

At the fault scarp the arroyo makes a right-angle and turns to flow north-south for about 30 m. This turn is caused by the massive Stage IV carbonate-impregnated colluvial wedge, which acts like a

huge mass of concrete placed in the path of the stream. The stream, after easily eroding through the sandy Camp Rice Formation, encountered the western edge of the cemented colluvial wedge as soon as the stream eroded past the fault plane. Unable to erode through the Stage IV carbonate, the stream turned north and flowed along the “back edge” of the colluvial wedge for about 30 m until it was able to break through and continue flowing east. This rather bizarre topography prevented us from observing a planar east-west section through the fault zone, so we used a backhoe to cut a ca. 4-5 m-high vertical wall (oriented east-west) along the natural arroyo bank in the footwall, across the fault zone, and into the hanging wall at the right-angle turn in the arroyo.

4.5.2 Stratigraphy

The footwall is underlain by 2 m of Jornada II gravels underlain by at least 4-5 m of Camp Rice Formation (base is not exposed). The Camp Rice Formation is almost entirely sand and is very well sorted and planar bedded. It appears to be a braided stream deposit similar to that deposited by the Rio Grande.

The hanging wall sequence is composed mainly of poorly-sorted, sandy-gravelly scarp-derived colluvium, but low in the section there are interbeds of alluvium.

4.5.3 Soils

The Jornada II gravels on the footwall carry a typical Stage III carbonate relict soil, similar to the one exposed in the footwall of the primary trench. The hanging wall deposits, in contrast, are impregnated with Stage IV carbonate to a depth of about 4 m below the surface (Fig. 20). This heavy carbonate impregnation all but masks the boundaries between the individual colluvial wedge and alluvial units, and makes it very difficult to determine the number of paleoearthquakes.

Why was the carbonate cementation of the hanging wall here so much greater than at the primary trench? We speculate that the presence of the Camp Rice Formation in the fault free face shed a large component of well-sorted sand into each colluvial wedge. This sand component made the colluvial wedge soft and porous, much more so than a gravel-dominated colluvial wedge. When infiltrating water began to carry dissolved carbonate into the wedge during pedogenesis, it was able to penetrate quite far downward and to pervasively plug the sandy wedges with carbonate. After each faulting event and colluvial deposition episode, the carbonate was able to completely penetrate each new colluvial wedge and then weld its Stage IV carbonate onto the top of the underlying Stage IV soil, eventually building up nearly a massive, nearly 4 m-thick K horizon.

4.5.4 Structure

The EFMF at the arroyo exposure is an east-dipping, down-to-the-east normal fault (Fig. 20). The fault zone is about 0.5 m wide at the base of the exposure, but widens upward. Near the ground surface the fault has fissured the Stage IV carbonate soil of the hanging wall, forming prominent fissures fills.

4.6 Interpretation of the Arroyo Exposure

We were unable to decipher much of a paleoseismic chronology from the arroyo exposure, for several reasons. First, the carbonate cementation made it very hard to distinguish individual stratigraphic units in the wedge. Second, the Stage IV carbonate cementation discouraged the use of luminescence

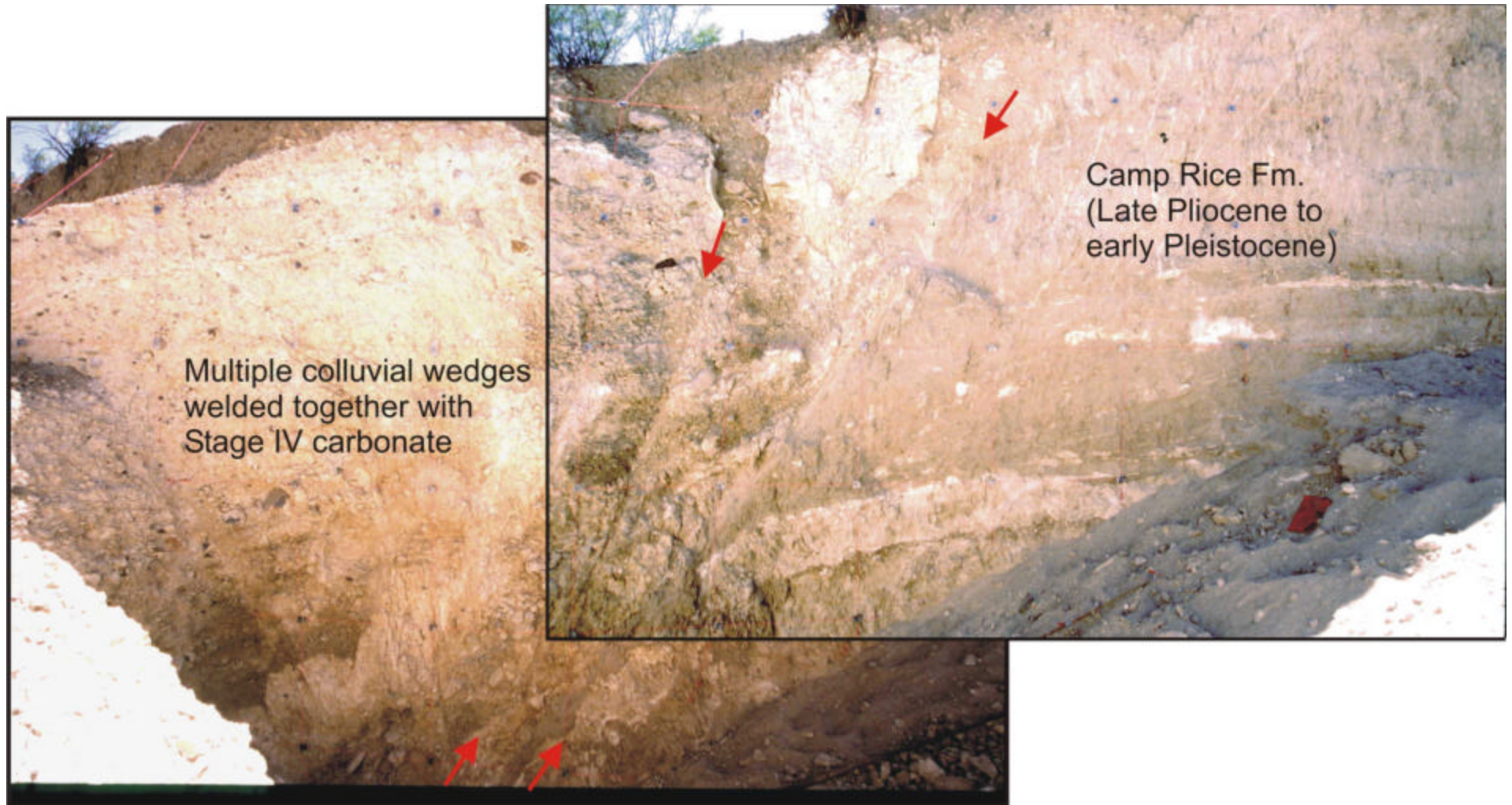


Fig. 20. Photomosaic of the arroyo exposure. Red arrows show the boundaries of the main fault zone. Red string lines are faintly visible, on a 1-m grid.

dating, because it would not be clear what was being dated. As a result, we did not collect any luminescence samples from the arroyo exposure, and thus have no age control. About all we can say is that the post-Jornada II vertical displacement at this site is >5.5 m.

5. SEISMIC SOURCE CHARACTERISTICS OF THE EAST FRANKLIN MOUNTAINS FAULT

Most of our seismic source characteristics come from evidence exposed in the primary trench. Only the long-term slip rates (post-Jornada I, post-Dona Ana) use scarp heights and displacements from other areas along the fault.

5.1 Number of Paleearthquake Events Interpreted

The primary trench has evidence for at least 4 events in the past 64 ka. The upper 3 events are expressed by unambiguous colluvial wedges and upward fault terminations. The colluvium from earliest event (Event W?) has been very deformed by subsequent events, but is also supported by upward fault terminations.

5.2 Displacement Per Event

As is typical on dip-slip faults, the measurement of displacement-per-event is hampered because correlative units are commonly absent across the fault. We employ a number of indirect techniques and assumptions to tease out displacement estimates for each of the 5 fault strands in each of the 4 displacement events (Table 5). For the latest 3 events, displacements in the trench vary from 3.0 m (Z), to 4.45 m (Y) to 2.95 m (X). The cumulative 3-event displacement is 10.4 m and the average is 3.45 m. However, if significant backtilting has affected the hanging wall, all these measurements overestimate the net vertical displacement across the entire EFMF.

5.3 Recurrence Interval Between Paleearthquakes

As can be seen in Table 5, the age control on each individual paleearthquake is rather poorly constrained. Given this fact, the best approach is to calculate an average recurrence between the past 4 events. The 4-event sequence spans 3 recurrence intervals. These 3 intervals post-date unit 13 (64.1 ± 5.7 ka) and end with event Z at 13-17 ka. Therefore, the 3 intervals span 41.4 to 56.8 ka, and have an average length of 13.8-18.9 ka (mean 16.4 ka).

5.4 Slip Rates

In section 4.4.4, we recommended a preferred slip rate of ca. 0.18 mm/yr be used for the primary trench site over the past 3 full seismic cycles. The slip rate over longer time periods can only be assessed from other areas, based on scarp heights across older (Jornada I, Dona Ana) geomorphic surfaces. Fig. 21 shows how Keaton and Barnes (1996) calculated their long-term slip rates. We have amended this figure to show our new slip rate from the primary trench (circle at lower left). In addition, we have indicated that their total displacements for Jornada I (250-400 ka) and Dona Ana (400-500 ka) surfaces are minimum estimates, as they state in their text. We mark those minimum displacement estimates with circles centered within each age range. These circles define a minimum slip rate of about 0.145 mm/yr over the past 500 ka.

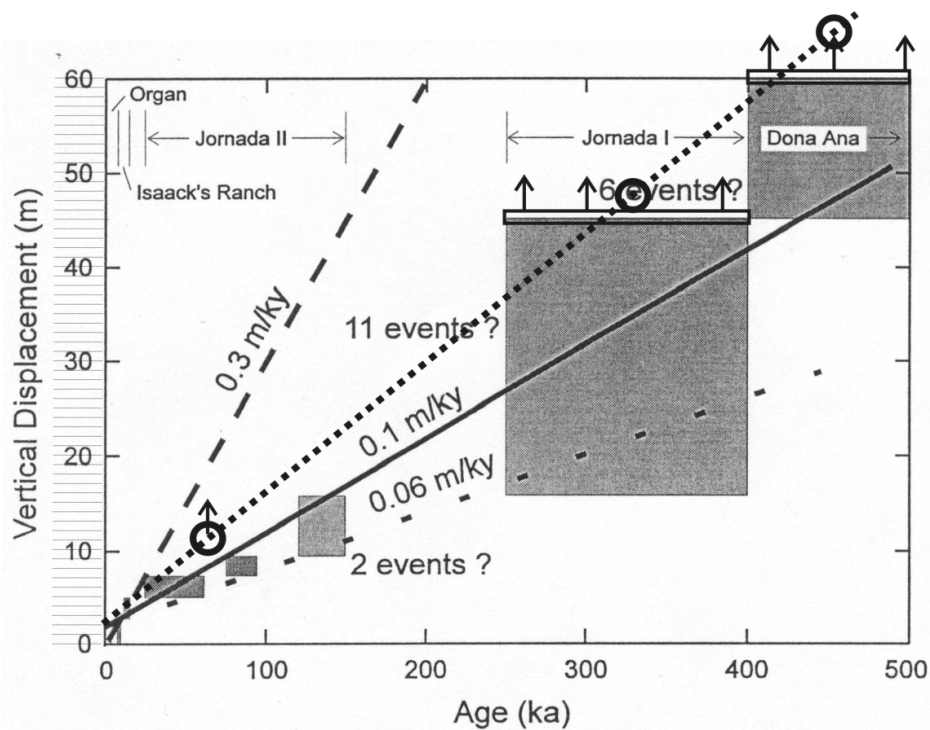


Fig. 21. Vertical displacement as a function of deposit age, adapted from Keaton and Barnes (1996). The minimum post-Dona Ana (400-500 ka) slip rate is defined the three circles, all of which are based on minimum displacements. Circle at lower left, $>11.2 \text{ m}/64 \text{ ka}$, from our primary trench; circle at center, $>45 \text{ m}/325 \text{ ka}$; circle at upper right, $>60 \text{ m}/450 \text{ ka}$. Dotted line shows reasonable minimum slip rate of 0.145 mm/yr .

Still, the unresolved matter of backtilting at all three calibration sites urges caution. We propose that the National Seismic Hazard Map use the 0.18 mm/yr slip rate as the maximum rate (perhaps weighted 35%) and the 0.145 mm/yr rate as the average (weighted 65%).

5.5 Implications for Regional Earthquake Hazard

The 2002 version of the National Seismic Hazard Map uses a slip rate of 0.10 mm/yr for the EFMF. We believe that rate is an underestimate, based on Keaton and Barnes (1996) making two erroneous conclusions: (1) overestimating the age of the displaced soils at the primary trench, and (2) forgetting that almost all of their displacement measurements for geomorphic surfaces of known age were minimum estimates, due to pervasive burial of the hanging walls. By using our higher slip rates of $0.145\text{-}0.18 \text{ mm/yr}$, the seismic hazard attributable to the EFMF will certainly increase in the National Map.

Due to the burgeoning population of the El Paso metropolitan area, this higher seismic hazard may trigger at least one additional study of the EFMF. That goal of that future study should be to pin down more accurately the age of the latest faulting event (Event Z). The age of Event Z determines the elapsed time since the latest earthquake, and the elapsed time is a very critical parameter in seismic hazard predictions that contain “memory” (i.e., calculations of conditional probability of rupture). The long-term average recurrence interval over the past 3 seismic cycles ($13.8\text{-}18.9 \text{ ka}$; mean 16.4 ka) will

probably not change much in future studies, unless they identify additional paleoearthquake events subsequent to 64 ka. However, the elapsed time as dated by us (13-17 ka) is approximately equal to the recurrence interval. Such a situation means that any calculation of conditional probability of future rupture is very sensitive to changes in the elapsed time.

The best way to obtain additional age estimates on Event Z is to trench single-event scarps farther south on the EFMF, say, near Trans Mountain Road. Mike Machette (pers. comm.) has located some potentially-trenchable, single-event fault scarps in that area, although coordination with Fort Bliss would be necessary. One advantage of trenching single-event scarps there for the sole purpose of dating Event Z is that the access is good, the trenches can be small, so the investigations can be relatively inexpensive and simple.

6. CONCLUSIONS

Our reexcavation of Keaton and Barnes' (1996) primary trench across the EFMF resulted in a different interpretation of fault displacement and age. Our luminescence age estimates, as well as sedimentology, indicate that the hanging-wall stratigraphy is only about half as old as assumed by Keaton and Barnes (1996), and only half as old as the footwall stratigraphic sequence. This is because the hanging wall of the fault scarp has been buried by younger alluvium, so the height of the scarp is considerably less than the net vertical displacement of the footwall stratigraphic units. We believe that this is a pervasive phenomenon along the EFMF, and has been generally unrecognized by previous workers, who equated scarp height with net displacement. We further believe that the reason for pervasive fluvial burial of the downthrown block is because the fault traces of the EFMF commonly lie 1 or more miles valleyward of the range front, and traverse a low-gradient piedmont. Thus the ephemeral streams have a low enough gradient that they tend to deposit alluvium and to fill up any tectonic "hole" (accommodation space) that might be created by normal faulting.

Because there is no correlation of strata across the fault, our net vertical displacement estimate is >11.2 m, compared to Keaton and Barnes (1996) estimate of 9.2-9.4 m. As a result of our larger displacement and much younger age, our calculated slip rate at the primary trench is 0.18 mm/yr, compared to their rate of 0.10 mm/yr.

Fault scarp heights and drillhole data provide first-approximations of vertical displacement across older datums (250-400 ka, 400-500 ka), but these approximations are also minimum values. The post-500 ka average slip rate based on these datums is 0.145 mm/yr.

We recommend that the next version of the National Seismic Hazard Map use the following slip rates for the EFMF: 0.145 mm/yr (weighted 65%) and 0.18 mm/yr (weighted 35%).

7. REFERENCES

Barnes, J.R., Keaton, J.R., Scherschel, C.A., and Monger, H.C., 1995, An integrated geomorphic and stratigraphic evaluation of late Quaternary earthquake activity along the East Franklin Mountains fault, El Paso, Texas [abs.], *in* Diversity in engineering geology and groundwater resources: Association of Engineering Geologists, 38th annual Meeting, Sacramento, California, October 2-8, 1995, p. 33.

Berger, G.W., 1994, Thermoluminescence dating of sediments older than ~100 ka: Quaternary Geochronology (Quaternary Science Reviews): 13: 445-455.

Buck, B.J., Kipp, J. M. Jr., Monger, H. C., 1998, Eolian Stratigraphy Of Intrabasinal Fault Depressions In The Northern Hueco And Southern Tularosa Basins: Evidence For Neotectonic Activity, New Mexico Geological Society 49th Guidebook, p. 79-86.

Cervený et al., 2006, A new strategy for analyzing the chronometry of constructed rock features in deserts: *Geoarcheology*, v. 21, no. 3, p. 281-303.

Collins, E. W., and Raney, J. A. 1990, Neotectonic history and structural style of the Campo Grande Fault, Hueco Basin, Trans-Pecos, Texas: The University of Texas at Austin, Bureau of Economic Geology contract report prepared for the Texas Low-Level Radioactive Waste Disposal Authority, 74 p.

Collins, E.W., and Raney, J.A., 1991, Tertiary and Quaternary structure and paleotectonics of the Hueco basin, trans-Pecos Texas and Chihuahua, Mexico: The University of Texas at Austin, Texas Bureau of Economic Geology Geological Circular 91-2, 44 p.

Collins, E. W., and Raney, J. A., 1993, Late Cenozoic faults of the region surrounding the Eagle Flat study area, northwestern Trans-Pecos Texas: University of Texas at Austin, Bureau of Economic Geology final contract report, prepared for Texas Low-Level Radioactive Waste Disposal Authority under Interagency Contract IAC (92-93)-0910, 74p.

Collins, E. W., and Raney, J. A., 1994, Tertiary and Quaternary tectonics of the Hueco bolson, Trans-Pecos Texas and Chihuahua, Mexico, in Keller, G. R., and Cather, S. M., eds., Basins of the Rio Grande rift: structure, stratigraphy, and tectonic setting: Boulder, Geological Society of America Special Paper No. 291, p. 265–282.

Collins, E. W., and Raney, J. A., 1997, Quaternary faults within intermontane basins of northwest Trans-Pecos Texas and Chihuahua, Mexico: The University of Texas at Austin, Bureau of Economic Geology Report of Investigations No. 245, 59 p.

Collins, E. W., and Raney, J. A., 2000, Geologic map of West Hueco Bolson, El Paso Region, Texas: The University of Texas at Austin, Bureau of Economic Geology, Miscellaneous Map No. 40, scale 1:100,000, 24-p. text.

Collins, E. W., Raney, J. A., Machette, M. N., Haller, K. M., and Dart, R. L., 1996, Map and data for Quaternary faults in West Texas and adjacent parts of Mexico: U.S. Geological Survey Open-File Report 96-002, ii + 74 p., 1 folded plate, scale 1:750,000.

Deutz, P., Montanez, I. P., Monger, H. C. & Morrison, J. (2001) Morphology and isotope heterogeneity of Late Quaternary pedogenic carbonates: Implications for paleosol carbonates as paleoenvironmental proxies. *Palaeogeography Palaeoclimatology Palaeoecology* 166, 293-317.

Gile, L. H., and Grossman, R.B., 1979, *The Desert Project Soil Monograph*: US Department of Agriculture, Soil Conservation Service, Washington, D.C., 984 p.

Goodell, P., 2001, A new family of Quaternary faults extending through El Paso, TX; Ciudad Juarez, Mexico; and southern New Mexico: *Geological Society of America, Abstracts with Programs*, v. 43, no. 6, p. 345

Harbour, R.L., 1972, *Geology of the northern Franklin Mountains, Texas and New Mexico*: U.S. Geological Survey Bulletin 1298, 129 p., 3 pls.

Hawley, J.W., 1996, Hydrogeologic framework of potential recharge areas in the Albuquerque Basin, central New Mexico, in Hawley, J.W. and Whitworth, T.M. (eds.), *Hydrogeology of potential recharge areas and hydrogeochemical modeling of proposed artificial-recharge methods in basin- and valley-fill aquifer systems, Albuquerque Basin, New Mexico*: New Mexico Bureau of Mines and Mineral Resources, Open-File Report 402-D, Chapter 1.

Imbrie, J., Boyle, E., Clemens, S., Duffy, A., Howard, W., Kukla, G., Kutzbach, J., Martinson, D., McIntyre, A., Mix, A., Molfino, B., Morley, J., Peterson, L., Pisias, N., Prell, W., Raymo, M., Sackleton, N., and Toggweiler, J., 1992: One the Structure and Origin of major Glaciation Cycles. 1. Linear responses to Milankovitch forcing: *Paleoceanography*, v. 7, p. 701-738.

Keaton, J.R, 1993, *Maps of potential earthquake hazards in the urban area of El Paso, Texas*: Technical report to U.S. Geological Survey, under Contract 1434-92-G-2171, July 28, 1993, 87 p.

Keaton, J.R, and Barnes, J.R, 1996, *Paleoseismic evaluation of East Franklin Mountains fault, El Paso, Texas*: Technical report to U.S. Geological Survey, under Contract 1434-94-G-2389, May 10, 1996, 45 p.

Keaton, J.R, Barnes, J.R, Scherschel, C. A., and Monger, H.C., 1995, *Evidence for episodic earthquake activity along the East Franklin Mountains fault, El Paso, Texas*: *Geological Society of America Abstracts with Programs*, v. 27, no. 4, p. 17.

Langford, R.P., 2001, *Segmentation of the Rio Grande alluvial surface and evolution of the Rio Grande rift*: *Geological Society of America, Abstracts with Programs*, v. 43, no. 6, p. 345

Lovejoy, E.M.P. and Hawley, J.W., 1987, *El Paso to New Mexico-Texas state line*, in Hawley, J.W. (ed.), *Guidebook to the Rio Grande rift in New Mexico and Colorado*: New Mexico Bureau of Mines and Mineral Resources, Circular 163, p.57-68.

Machette, M.N., 1978, *Dating Quaternary faults in the southwestern United States by using buried calcareous paleosols*: U.S. Geological Survey *Journal of Research*, v.6, p.369-381.

Machette, M.N., 1987, *Preliminary assessment of paleoseismicity at White Sands Missile Range, southern New Mexico: evidence for recency of faulting, fault segmentation, and repeat intervals for major earthquakes in the region*: U.S. Geological Survey Open-File Report 87-444, 46 p.

Machette, M.N., 1998, Contrasts between short- and long-term records of seismicity in the Rio Grande rift—important implications for seismic-hazard assessments in areas of slow extension: Utah Geol. Survey Spec. Pub., Salt Lake City, UT.

Machette, M.N., Personius, S.F., Kelson, K.I., Haller, K.M. and Dart, R.L., 1998, Map and data for Quaternary faults and folds in New Mexico: U.S. Geological Survey Open-File Report 98-521, 443 p.

McCalpin, J.P. (ed.), 1996a, Paleoseismology : Academic Press, NY, 583 pp.

McCalpin, J.P., 1996b, Paleoseismology of Extensional Tectonic Environments, Chapter 3 in McCalpin, J.P. (ed.), Paleoseismology: Academic Press, New York, p.85-146

McCalpin, J.P. and Berry, M.E., 1996, Soil catenas to estimate ages of movements on normal fault scarps, with an example from the Wasatch fault zone, Utah, USA: *Catena* 27:265-286.

Merriam, C. H. and Steineger, L. 1890. *Results of a biological survey of the San Francisco mountain region and the desert of the Little Colorado, Arizona: North American Fauna Report 3*. U.S. Department of Agriculture, Division of Ornithology and Mammalia, Washington, D.C., 136 pp.

Monger, H.C., 1993, Soil-geomorphic and paleoclimatic characteristics of the Fort Bliss maneuver areas, southern Mexico and western Texas: U.S. Army Air Defense Artillery Center, Directorate of the Environment, Historic and Natural Resources Report No. 10, 213 p.

Raney, J.A., and Collins, E.W., 1994a, Geologic map of the El Paso quadrangle, Texas: The University of Texas at Austin, [Texas] Bureau of Economic Geology Open-File Map, 1 sheet, scale 1:24,000.

Raney, J.A., and Collins, E.W., 1994b, Geologic map of the North Franklin Mountain quadrangle, Texas: The University of Texas at Austin, [Texas] Bureau of Economic Geology Open-File Map, 1 sheet, scale 1:24,000.

Richardson, G.B., 1909. Geologic atlas of the United States, El Paso Folio, Texas: U.S. Geological Survey, Washington, D.C., scale 1:125,000.

Scherschel, C., 1995, Quaternary geologic and geomorphic framework for neotectonic analysis of the northeastern Franklin Mountains, El Paso, Texas [abs.], *in* Diversity in engineering geology and groundwater resources: Association of Engineering Geologists, 38th Annual Meeting, Sacramento, California, October 2-8, 1995, p. 12-13.

Scherschel, C. A., Keaton, J.R, and Monger, H.C., 1995, Quaternary geologic and geomorphic framework for neotectonic analysis of the northeastern Franklin Mountains, El Paso, Texas: Geological Society of America Abstracts with Programs, v. 27, no. 4, p. 53.

Varney, R.A., 2004, Pollen and macrofossil analysis of sediments from a buried paleosol associated with the East Franklin Mountain fault, West Texas: unpublished consulting report submitted to GEO-HAZ Consulting, Inc., Crestone, CO, by Paleo Research Institute, Golden, CO, Jan. 2004, 8 p.

Wells, D.L. and K.J. Coppersmith, 1994, Empirical relationships among magnitude, rupture length, rupture area, and surface displacement: Bulletin of the Seismological Society of America, v. 84, p. 974-1002.

Wong, I. G. and 16 others, 1995, Seismic hazards evaluation of the Los Alamos National Laboratory, Final Report: submitted to Los Alamos National Laboratory by Woodward Clyde Federal Services, 25 Feb. 1995, 3 vols.

Wong, I. G. and Stepp, J.C., coordinators, 1998, Probabilistic seismic hazard analyses for fault displacement and vibratory ground motion at Yucca Mountain, Nevada-- Final Report: unpublished report submitted to the U.S. Department of Energy by the Civilian Radioactive Waste Management System Management and Operating Contractor, contract DE-AC04-94AL85000, 23 Feb. 1998, 3 volumes.

8. ACKNOWLEDGMENTS

This trenching study would not have been possible without the support and landowner permission granted by the El Paso Public Service Board, and the cooperation of its lessee, Bowen Ranch. Mr. Scott Reinert and Mr. Michael Fahy of the El Paso Water Utilities assisted in getting landowner permission. Mr. Bruce Seale of the Bowen Ranch made sure we could access the trench and didn't get stranded. Dr. Jeff Keaton and Mr. Jamie Barnes provided details of their earlier trenching and drilling study. Trenches were logged by J.P. McCalpin, L.C. Allen Jones, Deborah J. Green (GEO-HAZ), and Dr. Jose Hurtado (UTEP). This study was part of a collaborative study of Quaternary faulting in the El Paso metropolitan area, headed by Dr. Phil Goodell (UTEP). Drs. Diane Doser, Rich Langford, and Kate Miller (all UTEP) ran geophysical surveys across the fault scarp adjacent to the trench. Dr. Chris Andronicos (UTEP) discussed the tectonic setting of the area with us. Dr. Glenn Berger (Desert Research Institute, Reno, NV) collected the luminescence sampling and dated them. Mike Machette (USGS) blessed the trenches with his presence and made helpful suggestions. The trenches were excavated and backfilled by C.F. Jordan Co., El Paso., as coordinated by Mr. Mike Dooley and Mr. Mike Sullivan.

APPENDIX 1

DATABASE ENTRY FOR THE EAST FRANKLIN MOUNTAINS FAULT, from the U.S. Geological Survey's Quaternary Fault and Fold Database (<http://qfaults.cr.usgs.gov/faults/FMPro>)

Complete Report for East Franklin Mountains fault (Class A) No. 900

[Brief Report](#) || [Partial Report](#)

Compiled in cooperation with the Texas Bureau of Economic Geology and the New Mexico Bureau of Mines and Mineral Resources

citation for this record: Collins, E.W., and Machette, M.N., compilers, 1995, Fault number 900, East Franklin Mountains fault, in Quaternary fault and fold database of the United States, ver 1.0: U.S. Geological Survey Open-File Report 03-417, <http://qfaults.cr.usgs.gov>.

Synopsis:	This long fault forms a series of range-front scarps along the eastern base of the Franklin Mountains, primarily in West Texas. Studies of scarp morphology and reconnaissance mapping of faulted and unfaulted Quaternary deposits are the source of data for this fault. Results from trench investigations (Scherschel and others, 1995 #876; Keaton and others, 1995 #877; Barnes and others, 1995 #909; Keaton and Barnes, 1995 #944) were still preliminary at the time of this compilation. No significant work has been done on the fault in Mexico where its age and southern limit are poorly known.
	<p>Name Comments:</p> <p>Named by Machette (1987 #847). The fault extends from the northeast margin of the Franklin Mountains in southern New Mexico, south through Texas along the Franklin Mountains and across the Rio Grande along the southeast margin of the Sierra de Juárez in Chihuahua, Mexico.</p> <p>Number Comments:</p> <p>Referred to as fault 6 by Machette (1987 #847).</p>
State(s):	Texas New Mexico Chihuahua (Mexico)
County(s):	El Paso (Tex.) Dona Ana (N. Mex.)

<p>AMS sheet(s):</p>	<p>El Paso Las Cruces</p> <p>view map</p>
<p>Physiographic province(s):</p>	<p>Basin and Range province</p>
<p>Geologic setting:</p>	<p>Down-to-east, range-front fault bounding east side of the Franklin Mountains and Sierra de Juarez. This fault is part of a longer system that includes the Artillery Range [2051], Organ Mountains [2052], and San Andres [2053] faults in New Mexico.</p>
<p>Reliability of location:</p>	<p>Good. Compiled at 1:250,000 scale.</p> <p><i>Comments:</i> Location based on 1:250,000-scale map compiled from aerial photos and 1:24,000- to 1:250,000-scale maps of Sayre and Livingston (1945 #850), Morrison (1969 #848), Harbour (1972 #849), Machette (1987 #847), Collins and Raney (1991 #846; 1993 #852), Keaton (1993 #851), and Raney and Collins (1994 #872; 1994 #873).</p>
<p>Length (km):</p>	<p>52.7</p> <p><i>Comments:</i> The fault zone includes a main strand and several minor strands that have a cumulative trace length of 52.7 km. The southern end of the fault is not well mapped in Mexico.</p>
<p>Average strike:</p>	<p>N2°E</p>
<p>Sense of movement:</p>	<p>Normal</p> <p><i>Comments:</i> Sense of movement inferred from topography and from trench exposures of Keaton and Barnes (1995 #944).</p>
<p>Dip:</p>	<p>76°E</p>

	<p><i>Comments:</i> Dip measured in shallow excavation across northern end of fault (Keaton and Barnes, 1995 #944).</p>
<p>Paleoseismology studies:</p>	<p>Site 900-1. A single trench was excavated across the northern part of the fault in January 1995 by AGRA Earth and Environmental, on contract to the U.S. Geological Survey. Preliminary results of this trenching have been published by Keaton and others (1995 #877), Keaton and Barnes (1995 #944), Barnes and others (1995 #909), and Scherschel (1995 #916). All interpretations suggest 3 or 4 surface rupturing events since middle Pleistocene time (past 130 k.y.) on the basis of relations between colluvial materials, soils, and faults in the exposure. Two radiocarbon dates from colluvial wedges (10.9 ka and 15.6 ka) were reported by Keaton and Barnes (1995 #944). At the trench site, the Jornada II alluvium (late middle Pleistocene) is estimated to be offset vertically 8.5 m (Scherschel, 1995 #916) to as much as 9.8-10.6 m (Keaton and others, 1995 #877).</p>
<p>Geomorphic expression:</p>	<p>Distinct scarps are from 2 to 60 m high (Machette, 1987 #847; Collins and Raney, 1991 #846). Some scarps have compound slopes indicating young morphology superposed on older scarps. Steepest slope-angles are between 13° and 23° depending on height. Scarps are well dissected by streams draining the Franklin Mountains. The fault consists of multiple strands with scarps and grabens along the mountain front. Urbanization of El Paso and Juarez (Mexico) and young alluvium of the Rio Grande cover most of the southern part of the fault.</p>
<p>Age of faulted surficial deposits:</p>	<p>Mostly Quaternary alluvium along the eastern piedmont of the Franklin Mountains and Sierra de Juarez (Raney and Collins, 1994 #872; Raney and Collins, 1994 #873). Reconnaissance investigations of faulted alluvium indicate deposits at least as young as late Pleistocene are faulted (Machette, 1987 #847; Collins and Raney, 1991 #846; Collins and Raney, 1993 #852; Collins and Raney, 1994 #853; Scherschel and others, 1995 #876; Keaton and others, 1995 #877; Barnes and others, 1995 #909; Scherschel, 1995 #916). Holocene(?) or upper Pleistocene deposits have been faulted during the two most recent events. Colluvium shed from the scarp formed from the most recent event has a radiocarbon age of 10.9 ka (Keaton and Barnes, 1995 #944). The radiocarbon age of colluvium that was eroded from the scarp of the penultimate event is 15.6 ka (Keaton and Barnes, 1995 #944). These ages from colluvium indicate approximate minimum times for the two last scarp-forming events.</p>
<p>Year of historic</p>	

<p>deformation:</p>	
<p>Most recent prehistoric deformation:</p>	<p>Latest Quaternary (<15 ka)</p> <p><i>Comments:</i> Timing based on trenching by Keaton and Barnes (1995 #944) and morphometric analysis of small (single-event) scarps by Machette (1987 #847). Keaton and Barnes(1995 #944) reported that the likely age range for the most recent event is 8-12 ka based on scarp morphology and a radiocarbon date of 10.9 ka from scarp-derived colluvium. Additionally, soil studies by Monger (unpublished data, 1995) suggested that the oldest unfaulted deposits adjacent to the trench site are correlative to the Organ (Holocene) alluvium, which may be as old as 8 ka. However, Barnes and others (1995 #909), Keaton and others (1995 #877), Scherschel and others (1995 #876), and Scherschel (1995 #916) suggested that the most recent event is older than the Isaack’s Ranch alluvium, which is considered to be latest Pleistocene in age.</p>
<p>Recurrence interval:</p>	<p>9-22 k.y. (<130 ka)</p> <p><i>Comments:</i> The most recent work on the East Franklin Mountains fault suggests short episodes of faulting with displacement events recurring every 9-22 k.y., alternating with long stable intervals of 75-100 k.y. at least for the late Pleistocene (Keaton and others, 1995 #877; Barnes and others, 1995 #909). However, Scherschel (1995 #916) suggested recurrence intervals of about 30 k.y. for an unspecified period of time. Keaton and Barnes (1995 #944) used three probable slip rates and a characteristic displacement value to estimate average recurrence intervals of about 8-40 k.y. Collins and Raney (1993 #852) estimated that the average recurrence interval for large surface ruptures since middle Pleistocene time (<130 ka.) may be 15-30 k.y. These values are based on (1) estimated number of inferred large-displacement (1-to 2-m) surface ruptures since middle Pleistocene time, (2) assumption that faulted middle Pleistocene (Jornada I) deposits are approximately 250-500 ka, and (3) >25-32 m scarps on middle Pleistocene surfaces reflect the throw on fault.</p>
<p>Slip-rate category:</p>	<p>Between 0.2 and 1.0 mm/yr</p> <p><i>Comments:</i> The short-term slip rate is thought to be higher than the long-term rate due to clustering of events during late Quaternary time. The higher slip rate is used here to define the appropriate slip-rate category; although if a longer record is considered, the lowest slip-rate category would be indicated. Keaton and Barnes (1995 #944) suggested a slip rate of 0.3 mm/yr for the past 3 events (less than</p>

	<p>about 30 ka), but a long-term (<500 ka) slip rate of 0.1 mm/yr is also consistent with the data. Scherschel (1995 #916) suggested an even lower long-term slip rate of 0.065 mm/yr. A long-term slip rate of 0.25 mm/yr since middle Pleistocene time was inferred on the basis of >25-32 m of throw in the past 130 k.y. (Collins and Raney, 1993 #852).</p>
<p>Compiled or modified by and affiliation:</p>	<p>E.W. Collins, Bureau of Economic Geology, The University of Texas at Austin; Michael N. Machette, U.S. Geological Survey, 1995</p>
<p>References:</p>	<p>#909 Barnes, J.R., Keaton, J.R., Scherschel, C.A., and Monger, H.C., 1995, An integrated geomorphic and stratigraphic evaluation of late Quaternary earthquake activity along the East Franklin Mountains fault, El Paso, Texas [abs.] Diversity in engineering geology and groundwater resources: Association of Engineering Geologists, 38th Annual Meeting, Sacramento, California, October 2-8, 1995, p. 33.</p> <p>#846 Collins, E.W., and Raney, J.A., 1991, Tertiary and Quaternary structure and paleotectonics of the Hueco basin, trans-Pecos Texas and Chihuahua, Mexico: The University of Texas at Austin, [Texas] Bureau of Economic Geology Geological Circular 91-2, 44 p.</p> <p>#852 Collins, E.W., and Raney, J.A., 1993, Late Cenozoic faults of the region surrounding the Eagle Flat study area, northwestern trans-Pecos Texas: Technical report to Texas Low-Level Radioactive Waste Disposal Authority, under Contract IAC (92-93)-0910, 74 p.</p> <p>#853 Collins, E.W., and Raney, J.A., 1994, Impact of late Cenozoic extension on Laramide overthrust belt and Diablo Platform margins, northwestern trans-Pecos Texas, in Ahlen, J., Peterson, J., and Bowsher, A.L., eds., Geologic activities in the 90s: New Mexico Bureau of Mines and Mineral Resources Bulletin 150, p. 71-81.</p> <p>#849 Harbour, R.L., 1972, Geology of the northern Franklin Mountains, Texas and New Mexico: U.S. Geological Survey Bulletin 1298, 129 p., 3 pls.</p> <p>#851 Keaton, J.R., 1993, Maps of potential earthquake hazards in the urban area of El Paso, Texas: Technical report to U.S. Geological Survey, under Contract 1434-92-G-2171, July 28, 1993, 87 p.</p> <p>#944 Keaton, J.R., and Barnes, J.R., 1995, Paleoseismic evaluation of the East</p>

Franklin Mountains fault, El Paso, Texas: Technical report to U.S. Geological Survey, under Contract 1434-94-G-2389, December 1995.

#877 Keaton, J.R., Barnes, J.R., Scherschel, C.A., and Monger, H.C., 1995, Evidence for episodic earthquake activity along the East Franklin Mountains fault, El Paso, Texas: Geological Society of America Abstracts with Programs, v. 27, no. 4, p. 17.

#847 Machette, M.N., 1987, Preliminary assessment of paleoseismicity at White Sands Missile Range, southern New Mexico—Evidence for recency of faulting, fault segmentation, and repeat intervals for major earthquakes in the region: U.S. Geological Survey Open-File Report 87-444, 46 p.

#848 Morrison, R.B., 1969, Photointerpretive mapping from space photographs of Quaternary geomorphic features and soil associations in northern Chihuahua and adjoining New Mexico and Texas, in Córdoba, D.A., Wengerd, S.A., and Shomaker, J., eds., Guidebook of the Border Region: New Mexico Geological Society, 20th Field Conference, October 23-25, 1969, Guidebook, p. 116-129.

#872 Raney, J.A., and Collins, E.W., 1994, Geologic map of the El Paso quadrangle, Texas: The University of Texas at Austin, [Texas] Bureau of Economic Geology Open-File Map, 1 sheet, scale 1:24,000.

#873 Raney, J.A., and Collins, E.W., 1994, Geologic map of the North Franklin Mountain quadrangle, Texas: The University of Texas at Austin, [Texas] Bureau of Economic Geology Open-File Map, 1 sheet, scale 1:24,000.

#850 Sayre, A.N., and Livingston, P., 1945, Ground-water resources of the El Paso area, Texas: U.S. Geological Survey Water-Supply Paper 919, 190 p.

#916 Scherschel, C., 1995, Quaternary geologic and geomorphic framework for neotectonic analysis of the northeastern Franklin Mountains, El Paso, Texas [abs.] Diversity in engineering geology and groundwater resources: Association of Engineering Geologists, 38th Annual Meeting, Sacramento, California, October 2-8, 1995, p. 12-13.

#876 Scherschel, C.A., Keaton, J.R., and Monger, H.C., 1995, Quaternary geologic and geomorphic framework for neotectonic analysis of the northeastern Franklin Mountains, El Paso, Texas: Geological Society of America Abstracts with Programs, v. 27, no. 4, p. 53.

APPENDIX 2—Structure of the Franklin Mountains (from Richardson, 1909)

(numbers in parentheses indicate page numbers in the original USGS Folio of the El Paso Sheet)

(56)

STRUCTURE OF THE EL PASO DISTRICT.
GENERAL OUTLINE.

The main structural features of the El Paso district may be summarized as follows: The long, narrow Franklin Range, rising 3000 feet above broad lowlands, resembles a "basin range" fault block of west ward-dipping rocks, but it differs from the type by being part of a long chain of ranges and by being complexly faulted internally. The Hueco Mountains in the main form a monocline of low eastward dip along the western border of which the rocks have been disturbed. In the northern part of the quadrangle the strata in the belt of low outlying bills west of the Hueco Mountains dip westward, marking an unsymmetrical anticline; farther south more complex conditions are indicated by dips in various directions. In the Hueco Bolson the deep cover of unconsolidated material conceals the structure of the underlying rocks. Possibly a large part of the area is underlain by practically flat-lying beds which are faulted near the western margin of the bolson along the eastern base of the Franklin Mountains. (See fig. 11.)

FRANKLIN MOUNTAINS.

The structure of the Franklin Mountains viewed from a distance appears simple. The strata strike parallel to the trend of the range and dip westward at steep angles. But the simplicity is only apparent, for the distribution of the rocks shows that the range is traversed by many faults. As a whole the

(58)

long, narrow mountain belt bordered by broad waste-covered deserts, the western slopes coinciding with the dip of the rocks and the steeper eastern face exposing eroded edges of the strata, presents the general appearance of an eroded fault block of the basin-range type.

Two prominent sets of almost vertical joints are developed in the rocks throughout the range, one parallel and the other transverse to the trend of the mountains. The planes are close together and in general are best defined in the sediments, but they are also well developed in the igneous rocks, especially in the granite.

The Franklin Range is broken by normal faults into several blocks, the most prominent of which, for convenience of description, have been given the following names: Hueco, Anthony, Newman, Cassiterite, North Franklin, Central Franklin, South Franklin, Taylor, and McKilligan; these are shown in figure 12. Some of the faults bear in general parallel to the trend of the range; there are also several transverse dislocations, and the strike of a few is distinctly curved. The distribution of the rocks is such that the presence of the faults is readily determined, and the recognition of like horizons on both sides of the dislocations in several places enables an approximate determination of the amount of the displacement.

The Franklin Range lies between two major longitudinal dislocations which separate it from the Hueco block on the east and the Anthony block on the west. On the east the position of the hypothetical fault along the base of the range is completely concealed by wash. On the west the dislocation consists of two parallel faults at the base of the range between the foothills and the main mountain mass. These faults can be followed for several miles and probably border the entire range. The greatest displacement appears in the central part of the range, where the Hueco limestone and the rhyolite porphyry are closely associated, indicating a throw of more than 2500 feet. Farther north, near the State boundary, the position of the faults is concealed by an expanse of wash about a mile wide on both sides of which Hueco limestone outcrops,

(60)

indicating, that the throw has increased. Six miles north of El Paso, along the southern continuation of the fault zone, the Hueco limestone lies adjacent to the El Paso limestone. The easternmost of these parallel faults along the western base of the mountains has a, relatively small throw, indicated by steeply tilted lower Paleozoic strata abutting against the rhyolite porphyry, but farther north the throw is reversed and increased in amount by the cross fault which separates the North Franklin and Central Franklin blocks and brings the Bliss sandstone into contact with the Hueco limestone.

These major longitudinal dislocations do not affect the continuity of the strata in the main Franklin Range, which is separated by faults into seven principal blocks and other smaller ones. The sections across the range given in figure 13 show the structural relations. Beginning at the north and proceeding southward the main dislocations are as follows:

The rocks in the ridge trending south of east next to the Texas-New Mexico boundary have been dropped down on the north relative to those on the south by a transverse fault which separates the Newman from the North Franklin and Cassiterite blocks. The ridge is composed chiefly of Hueco limestone, the normal position of which is on the western slope of the range at the top of the Paleozoic section, but in their present position the strata of the ridge, if continued across the fault, would strike into the El Paso, Bliss, and Lanoria formations. The cross ridge itself is broken by two parallel north-south faults. Near the east end Hueco limestone abuts against El Paso limestone, the former dipping almost due west and the latter southwest. The relative downthrow is on the west, but the amount of displacement can not be measured. The other fault cuts the Hueco limestone.

One of the main faults of the range is the longitudinal one which separates the North Franklin and Cassiterite blocks. The North Franklin block includes the main northern ridge, which is composed of the normal sequence of strata from the Cambrian to the Carboniferous inclusive. The Cassiterite block is relatively downthrown and forms the eastern foothills

(62)

in the northern part of the range. The position of the fault plane is concealed by a great mass of granite which apparently is genetically connected with the faulting. This fault is shown by the presence in the Cassiterite block of the same strata which appear higher up in the range in the North Franklin block, so that the strata of the Cassiterite block appear to dip beneath those of the other block. The greatest throw is in the vicinity of the tin prospects 12 miles north of El Paso, where the Fusselman and Montoya limestones have been displaced more than 3000 feet. The fault decreases in intensity toward the north, and in the transverse ridge 2 miles south of the State boundary the displacement of the El Paso limestone and the Bliss sandstone amounts to about 1300 feet. A subsidiary parallel displacement is indicated by the presence of the Bliss sandstone and the El Paso limestone on the knob about a mile southeast of the tin prospects.

An important transverse fault separates the North Franklin and Cassiterite blocks on the north from the Central Franklin block on the south. This fault crosses the range at the pass near Cottonwood Springs and, like the one just discussed, is associated with granite. It causes the Paleozoic strata of the northern and relatively downthrown blocks to strike toward pre-Cambrian rocks of the Central Franklin block. There is a secondary parallel dislocation about half a mile to the north, where the relative downthrow is also on the north and different Paleozoic formations are in contact on opposite sides of the displacement.

The central and southern parts of the range are composed of four main blocks-the Central Franklin, South Franklin, Taylor, and McKilligan. The main fault extends along the eastern flank of the ridge north of El Paso and passing west of the high summit in the south-central part of the range, curves northeastward and extends down the valley of Fusselman Canyon. This displacement is plainly marked. At its south end the fault extends between the South Franklin and McKilligan blocks, which are separated by a belt of granite occurring along the zone of dislocation. The Bliss sandstone and the El Paso,

(63)

Fusselman, and Montoya limestones outcrop in the South Franklin block and form the main southern ridge of the range. These limestones are repeated in the McKilligan block, which includes a wedge-shaped area of low hills at the

eastern base of the mountains. The displacement here amounts to about 2300 feet, but toward the north it decreases somewhat. North of the wash-filled McKilligan Canyon what apparently is the continuation of this fault separates the Central Franklin and Taylor blocks. On following the fault up the mountain the Bliss sandstone is first found in juxtaposition with the Montoya limestone, and at the summit the El Paso is in contact with the Fusselman limestone. In this locality a prominent breccia is developed that is well marked at the head of the valley in which the Bliss sandstone outcrops. There a zone at least 20 feet wide is composed of indurated breccia consisting of angular fragments of limestone ranging from small bits up to pieces a foot in diameter. Beyond the summit, where the fault plane turns eastward, the displacement, although concealed by debris, is well shown by the fact that the lower part of the pre-Cambrian rhyolite porphyry and the Lanoria quartzite in the Central Franklin block north of Fusselman Canyon strike toward the Paleozoic and upper pre-Cambrian rocks in the relatively downthrown Taylor block to the southeast.

The blocks on both sides of the fault that has just been described have been disturbed by subsidiary movements. The southern part of the Taylor block is separated from the McKilligan block by a fault of 700 feet displacement, whereby the strata are repeated, the downthrow as usual being on the east. (See geologic map and fig. 14.) Two minor faults striking northeastward, as shown on the map, break the continuity of the strata in the outlying ridge northwest of Fort Bliss. A greater displacement, amounting to more than 1000 feet, is indicated by the small outlying area of El Paso limestone at the extreme eastern base of this ridge. At the southwest end of the range a small wedge-shaped block in which the Hueco limestone outcrops enters the South Franklin block, the Fusselman and Montoya limestones outcropping west of it.

The abrupt termination of the Franklin Mountains at El Paso indicates a transverse fault. The rocks of these mountains are the southernmost Paleozoic strata so far discovered in that longitude in North America and farther south only Mesozoic and younger rocks are known. R. T. Hill has suggested that this probable fault is in line with the northwest-southeast system of displacements by which the older north-south faults of the basin ranges are intersected in many places in southwestern United States and northern Mexico.

APPENDIX 3
RADIOCARBON DATES

FROM: Darden Hood, Director (mailto:mailto:dhood@radiocarbon.com)
(This is a copy of the letter being mailed. Invoices/receipts follow only by mail.)

January 21, 2004

Dr. James McCalpin
GEO-HAZ Consulting, Incorporated
P.O. Box 837
600 East Galena Avenue
Crestone, CO 81131
USA

RE: Radiocarbon Dating Results For Samples EPC2, EPC6, EPC8

Dear Jim:

Enclosed are the radiocarbon dating results for three samples recently sent to us. They each provided plenty of carbon for accurate measurements and all the analyses went normally. As usual, the method of analysis is listed on the report with the results and calibration data is provided where applicable.

As always, no students or intern researchers who would necessarily be distracted with other obligations and priorities were used in the analyses. We analyzed them with the combined attention of our entire professional staff.

If you have specific questions about the analyses, please contact us. We are always available to answer your questions.

Our invoice is enclosed. Please, forward it to the appropriate officer or send VISA charge authorization. Thank you. As always, if you have any questions or would like to discuss the results, don't hesitate to contact me.

Sincerely,



Dr. James McCalpin

Report Date: 1/21/2004

GEO-HAZ Consulting, Incorporated

Material Received: 12/15/2003

Sample Data	Measured Radiocarbon Age	¹³ C/ ¹² C Ratio	Conventional Radiocarbon Age(*)
Beta - 186911 SAMPLE : EPC2 ANALYSIS : AMS-Standard delivery MATERIAL/PRETREATMENT : (carbonate sediment): none	29180 +/- 260 BP	-4.2 o/oo	29520 +/- 260 BP
Beta - 186912 SAMPLE : EPC6 ANALYSIS : Radiometric-Standard delivery (bulk low carbon analysis on sediment) MATERIAL/PRETREATMENT : (carbonate sediment): none 2 SIGMA CALIBRATION : (result is outside of the calibration range)	23190 +/- 160 BP	-4.8 o/oo	23520 +/- 160 BP
Beta - 186913 SAMPLE : EPC8 ANALYSIS : Radiometric-Standard delivery (bulk low carbon analysis on sediment) MATERIAL/PRETREATMENT : (carbonate sediment): none 2 SIGMA CALIBRATION : Cal BC 9270 to 9120 (Cal BP 11220 to 11070) AND Cal BC 9000 to 8890 (Cal BP 10950 to 10840) Cal BC 8880 to 8840 (Cal BP 10830 to 10800)	9410 +/- 70 BP	-5.8 o/oo	9720 +/- 70 BP

CALIBRATION OF RADIOCARBON AGE TO CALENDAR YEARS

(Variables: C13/C12=-5.8;lab. mult=1)

Laboratory number: **Beta-186913**

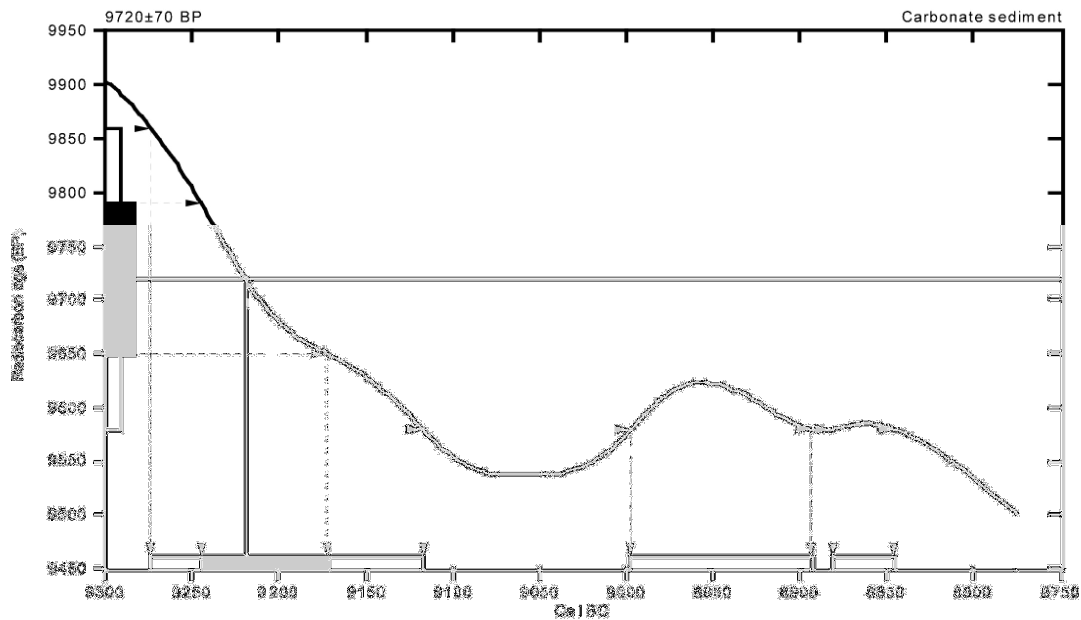
Conventional radiocarbon age: **9720±70 BP**

2 Sigma calibrated results: **Cal BC 9270 to 9120 (Cal BP 11220 to 11070) and
(95% probability) Cal BC 9000 to 8890 (Cal BP 10950 to 10840) and
Cal BC 8880 to 8840 (Cal BP 10830 to 10800)**

Intercept data

Intercept of radiocarbon age
with calibration curve: **Cal BC 9220 (Cal BP 11170)**

1 Sigma calibrated result: **Cal BC 9240 to 9170 (Cal BP 11200 to 11120)**
(68% probability)



References:

- Database used*
Intcal98
- Calibration Database*
Editorial Comment
Stuiver, M., van der Plicht, H., 1998, Radiocarbon 40(3), p11-15
- INTCAL98 Radiocarbon Age Calibration*
Stuiver, M., et al., 1998, Radiocarbon 40(3), p1041-1053
- Mathematical*
A Simplified Approach to Calibrating C14 Dates
Tolmo, A. S., Vogel, J. C., 1993, Radiocarbon 35(2), p317-322

Beta Analytic Radiocarbon Dating Laboratory

4921 S.W. 74th Court, Miami, Florida 33155 • Tel: (305)687-5167 • Fax: (305)613-0294 • E-Mail: beta@radiocarbon.com

APPENDIX 4

Pollen analysis of Unit 13Kb3 from Primary Trench

POLLEN AND MACROFOSSIL ANALYSIS OF SEDIMENTS FROM A BURIED PALEOSOL
ASSOCIATED WITH THE EAST FRANKLIN MOUNTAIN FAULT, WEST TEXAS

By

R.A. Varney

With Assistance from
Laura Beuthel
and
Kathryn Puseman

Paleo Research Institute
Golden, Colorado

Paleo Research Institute Technical Report 04-05

Prepared For

GEO-HAZ Consulting, Inc.
Crestone, Colorado

January 2004

INTRODUCTION

The East Franklin Mountain fault is located in the area of El Paso, Texas. A paleoseismic trench across the fault encountered at least three buried soils. The third of these, 13Kb3, radiocarbon dated to $29,520 \pm 260$ BP, was sampled as suspected cienega deposits in order to assist in determining vegetation in the area during the time of development of this soil. Samples were analyzed for pollen and plant macrofossils. Modern vegetation on the alluvial fans in the area consists of sparse cactus.

METHODS

Pollen

A chemical extraction technique based on flotation is the standard preparation technique used in this laboratory for the removal of the pollen from the large volume of sand, silt, and clay with which they are mixed. This particular process was developed for extraction of pollen from soils where preservation has been less than ideal and pollen density is low.

Hydrochloric acid (10%) was used to remove calcium carbonates present in the soil, after which the samples were screened through 150 micron mesh. The samples were rinsed until neutral by adding water, letting the samples stand for 2 hours, then pouring off the supernatant. A small quantity of sodium hexametaphosphate was added to each sample once it reached neutrality, then the beaker was again filled with water and allowed to stand for 2 hours. The samples were again rinsed until neutral, filling the beakers only with water. This step was added to remove clay prior to heavy liquid separation. At this time the samples are dried then gently pulverized. Sodium polytungstate (density 2.1) was used for the flotation process. The samples were mixed with sodium polytungstate and centrifuged at 2000 rpm for 5 minutes to separate organic from inorganic remains. The supernatant containing pollen and organic remains is decanted. Sodium polytungstate is again added to the inorganic fraction to repeat the separation process. The supernatant is decanted into the same tube as the supernatant from the first separation. This supernatant is then centrifuged at 2000 rpm for 5 minutes to allow any silica remaining to be separated from the organics. Following this, the supernatant is decanted into a 50 ml conical tube and diluted with distilled water. These samples are centrifuged at 3000 rpm to concentrate the organic fraction in the bottom of the tube. After rinsing the pollen-rich organic fraction obtained by this separation, all samples received a short (10-15 minute) treatment in hot hydrofluoric acid to remove any remaining inorganic particles. The samples were then acetolated for 3 minutes to remove any extraneous organic matter.

A light microscope was used to count the pollen to a total of 50 pollen grains at a magnification of 500x. Pollen preservation in these samples varied from excellent to fair. Comparative reference material collected at the Intermountain Herbarium at Utah State University and the University of Colorado Herbarium was used to identify the pollen to the family, genus, and species level, where possible.

Pollen diagrams are produced using Tilia, which was developed by Dr. Eric Grimm of the Illinois State Museum. Pollen concentrations are calculated in Tilia using the quantity of sample

processed (cc), the quantity of exotics (spores) added to the sample, the quantity of exotics counted, and the total pollen counted.

Indeterminate pollen includes pollen grains that are folded, mutilated, and otherwise distorted beyond recognition. These grains are included in the total pollen count, as they are part of the pollen record.

Macrofloral

The macrofloral sample was floated using a modification of the procedures outlined by Matthews (1979). The sample was added to approximately 3 gallons of water, then stirred until a strong vortex formed. The floating material (light fraction) was poured through a 150 micron mesh sieve. Additional water was added and the process repeated until all floating material was removed from the sample (a minimum of 5 times). The material which remained in the bottom (heavy fraction) was poured through a 0.5 mm mesh screen. The floated portions were allowed to dry.

The light fraction was weighed, then passed through a series of graduated screens (US Standard Sieves with 2 mm, 1 mm, 0.5 mm and 0.25 mm openings) to separate charcoal debris and to initially sort the seeds. The contents of each screen were then examined. Charcoal pieces larger than 2 mm in diameter were separated from the rest of the light fraction and the total charcoal weighed. A representative sample of these charcoal pieces was broken to expose a fresh cross-section and examined under a binocular microscope at a magnification of 70x. The weights of each charcoal type within the representative sample also were recorded. The material which remained in the 2 mm, 1 mm, 0.5 mm, and 0.25 mm sieves was scanned under a binocular stereo microscope at a magnification of 10x, with some identifications requiring magnifications of up to 70x. The material which passed through the 0.25 mm screen was not examined. The heavy fraction was scanned at a magnification of 2x for the presence of botanic remains. Remains from the light and heavy fractions were recorded as charred and/or uncharred, whole and/or fragments. The term "seed" is used to represent seeds, achenes, caryopses, and other disseminules. Macrofloral remains were identified using manuals (Martin and Barkley 1961; Musil 1963; Schopmeyer 1974) and by comparison with modern and archaeological references.

Samples from archaeological sites commonly contain both charred and uncharred remains. Many ethnobotanists use the basic rule that unless there is a specific reason to believe otherwise, only charred remains will be considered prehistoric (Minnis 1981:147). Minnis (1981:147) states that it is "improbable that many prehistoric seeds survive uncharred through common archaeological time spans." Few seeds live longer than a century, and most live for a much shorter period of time (Harrington 1972; Justice and Bass 1978; Quick 1961). It is presumed that once seeds have died, decomposing organisms act to decay the seeds. Sites in caves, water-logged areas, and in very arid areas, however, may contain uncharred prehistoric remains. Interpretation of uncharred seeds to represent presence in the prehistoric record is considered on a sample-by-sample basis. Extraordinary conditions for preservation are required.

DISCUSSION

The pollen record from this soil reflects a vegetation community very different from the sparse cactus cover described for the area (Figure 1 and Table 2). *Acacia* and *Prosopis* pollen represent acacia and mesquite trees growing in the area. *Pinus* pollen is low density, buoyant and can be transported long distances on the wind, thus likely indicating pine trees in distant mountains rather than the local area. *Quercus* pollen was the dominant type noted and reflects the local growth of oaks. *Artemisia* pollen represents sagebrush growing in the area. High-spine Asteraceae pollen noted in the sample likely indicates shrubby members of the sunflower family such as rabbitbrush. *Cereus* and *Echinocereus* pollen were present in moderate quantities and indicate the local growth of columnar cactus and hedgehog or strawberry cactus. Chenopodiaceae pollen was well represented in the sample and indicates the growth of shrubby or herbaceous members of the goosefoot family and/or amaranth. Lamiaceae pollen was noted in the sample in a low frequency and reflects the local growth of members of the mint family. Mints are usually associated with stable moisture, and the presence of Lamiaceae pollen in this sample indicates that water was available in the area. *Larrea* pollen represents creosote bush growing in the area. *Larrea* pollen is almost always under-represented in the pollen record, so its presence in this sample indicates that creosote bush was well represented in the local plant community. Poaceae pollen noted in the sample reflects grasses in the area. *Polygonum accuminatum* pollen represents knotweed as part of the local vegetation. Rhamnaceae pollen indicates members of the buckthorn family as part of the shrubby plant vegetation. Rosaceae pollen indicates that a member or members of the rose family occurred among the local vegetation. *Typha* pollen indicates the growth of cattails and further represents standing water in the area.

No plant remains were observed in the macrofloral analysis, precluding adding supportive information from that database.

SUMMARY AND CONCLUSIONS

The pollen assemblage noted in the sample suggests a bosque plant community rather than a cienega. These communities are typically dense stands of mesquite and acacia trees with oaks well represented in the higher elevations. Given that this soil was being developed ~30,000 years ago during a period of colder climate, a mixed oak/mesquite bosque would not be unexpected if moisture were available. The presence of mints and cattails indicates that not only was subsurface water available, but that there was open water or perennially marshy conditions in the area.

TABLE 1
PROVENIENCE DATA FOR SAMPLES FROM SITE EAST FRANKLIN MOUNTAINS FAULT

Sample No.	Unit No.	Depth (cmbs)	Provenience/ Description	Analysis
1	13Kb3		Suspected cienega (marsh) deposit	Pollen Macrofloral

TABLE 2
 POLLEN TYPES OBSERVED IN SAMPLES FROM EAST FRANKLIN MOUNTAINS FAULT

Scientific Name	Common Name
ARBOREAL POLLEN:	
<i>Acacia</i>	Acacia
<i>Pinus</i>	Pine
<i>Quercus</i>	Oak
NON-ARBOREAL POLLEN:	
Asteraceae:	Sunflower family
<i>Artemisia</i>	Sagebrush
High-spine	Includes aster, rabbitbrush, snakeweed, sunflower, etc.
Cactaceae:	Cactus family
<i>Cereus-type</i>	Columnar cereus cactus
<i>Echinocereus</i>	Hedgehog cactus, Strawberry cactus
Cheno-am	Includes the goosefoot family and amaranth
Lamiaceae	Mint family
Poaceae	Grass family
<i>Polygonum accuminatum</i>	Knotweed
Rhamnaceae	Buckthorn family
Rosaceae:	Rose family
<i>Typha angustifolia</i>	Cattail
Indeterminate	Too badly deteriorated to identify

REFERENCES CITED

- Harrington, H.D.
1972 *Western Edible Wild Plants*. The University of New Mexico Press, Albuquerque, New Mexico.
- Justice, Oren L. and Louis N. Bass
1978 *Principles and Practices of Seed Storage*. Agriculture Handbook ed 506. U.S. Department of Agriculture, Washington D.C.
- Martin, Alexander C. and William D. Barkley
1961 *Seed Identification Manual*. University of California, Berkeley, California.
- Matthews, Meredith H.
1979 Soil Sample Analysis of 5MT2148: Dominguez Ruin, Dolores, Colorado. Appendix B. In *The Dominguez Ruin: A McElmo Phase Pueblo in Southwestern Colorado*, edited by A. D. Reed. Bureau of Land Management Cultural Resource Series. vol. 7. Bureau of Land Management, Denver, Colorado.
- Minnis, Paul E.
1981 Seeds in Archaeological Sites: Sources and Some Interpretive Problems. *American Antiquity* 46(1):143-152.
- Musil, Albina F.
1963 *Identification of Crop and Weed Seeds*. Agricultural Handbook no. 219. U.S. Department of Agriculture, Washington D.C.
- Quick, Clarence R.
1961 How Long Can a Seed Remain Alive? In *Seeds, the Yearbook of Agriculture*, edited by A. Stefferud, pp. 94-99. U.S. Government Printing Office, Washington D.C.
- Schopmeyer, C.S.
1974 *Seeds of Woody Plants in the United States*. Agricultural Handbook No. 450. U.S. Department of Agriculture, Washington, D.C.

FIGURE 1. POLLEN DIAGRAM FOR THE EAST FRANKLIN MOUNTAINS FAULT.

